UiT
THE ARCTIC UNIVERSITY OF NORWAY

Faculty of Engineering Science and Technology

Modular Design of Integrated Duct Fan Quadrotor Structure

—

Sven Ole Hoff and André Rones

Master's thesis in Engineering Design June 2017

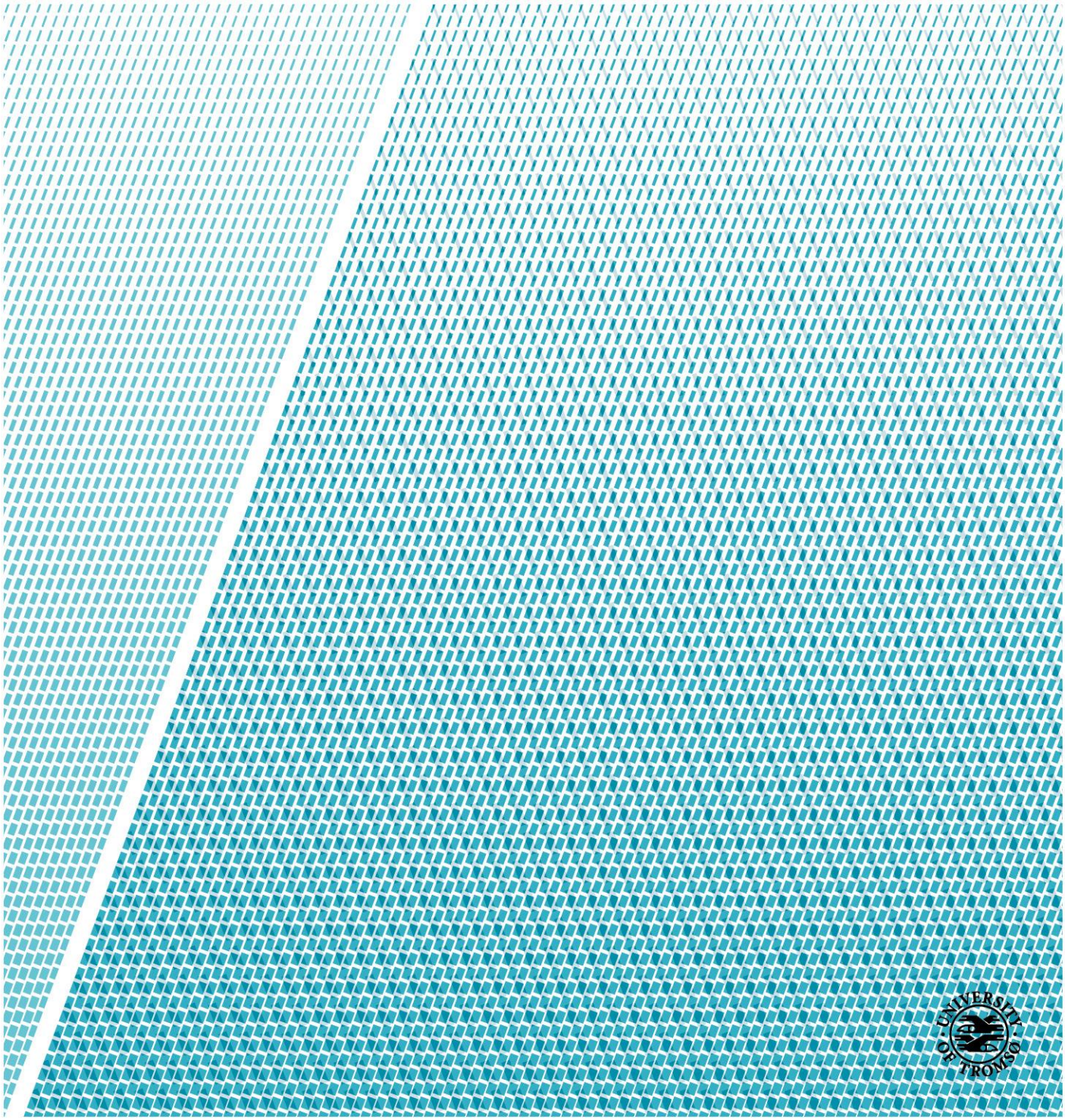

Master of Science

UiT – The Arctic University of Norway in Narvik

Lodve Langes gate 2, 8514 Narvik
Postbox 385
8505 NARVIK
Tlf: 77 64 40 00

Title: Modular Design of Integrated Duct Fan Quadrotor Structure	*Date:* 6/6/2017
Authors: Sven Ole Hoff & André Rones	*Classification:* *Open*
Department: Department of Computer Science and Computational Engineering	*Pages: 41* *Attachments: 6*
Faculty: Faculty of Engineering Science and Technology	
Study Program: Engineering Design	
Supervisors: Guy Beeri Mauseth & Per Johann Nicklasson	

Keywords:

Ducted fan, modular, lightweight, quadrotor.

Abstract:

This thesis will continue the work done by Sethuram Balakrishnan in his master thesis "Duct fanned shielding design for quadrotors". It includes studies of integrating Balakrishnan's solution to the outer structure of the DJI Flame Wheel F450 Quadrotor in order to save weight. A report with preliminary work will cover investigation of existing solutions and technology, setting design requirements and explore standards given by the government. The goal was to reduce mass from the previous design, make it modular and retain the mechanical properties of the quadrotor. Concepts were created and evaluated with the systematic design process explained by Nigel Cross in his book "engineering design methods". Materials was selected in CES by maximizing the material index for a low mass/stiff construction. Numerical analysis in Inventor was done to verify the structural integrity of the model, and a prototype was constructed to give a real perspective of the model. The process produced a final design that was 500g lighter than Balakrishnan's design, modular and cost effective. This means a 43,5% reduction in mass. The results in theory are interesting, and if results from physical testing corresponds, it will possibly have implications for production of drones with a need for increased thrust and protected propellers.

Acknowledgments

This thesis was carried out at the Faculty of Engineering Science and Technology at UiT – The Arctic University of Norway, campus Narvik under the supervision of Guy Beeri Mauseth and Per Johan Nicklasson. We want to thank our supervisors for the guidance and encouragements throughout the project. As relatively new to the quadrotor and drone technology we want to thank Tor-Alexander Johansen, contact person at the UiT department of electrotechnology, which helped us with problems and gave us ideas during the project. Erlend Bjørk has helped us with 3D printing and shared his experience within the 3D printing technology with us, we are grateful for his help. A thank to our fellow students for discussing the aspects of our project with us and in that way helped and inspired us. At last we want to thank UiT – The Arctic University of Norway for letting us use the facilities at the school.

Table of Contents

List of tables

List of Figures

Abbreviations

CA	Cellulose Acetate
CAD	Computer Assisted Design
CES	Cambridge Engineering Selector
LD	Low Density
MD	Medium Density
RPF	Rigid Polymer Foam
PA	Polyamid
PCB	Printed Circuit Board
PLA	Polylactic Acid
RPM	Revolutions Per Minute
VLD	Very Low Density
UiT	Universitetet I Tromsø

1 Introduction

1.1 Background

This master thesis is based on the work of Sethuram Balakrishnan in his master thesis "Duct fanned shielding design for quadrotors" from 2016 in cooperation with UiT. Balakrishnan came up with a solution which gave thrust increase and rotor shielding for the quadrotor DJI Flame wheel F450. The dronelab at UiT in Narvik has a goal to make the drone completely autonomous. That means it will fly all on its own without any manual control. This leads to an increased demand for safety, both for the drone itself and the environment. In the previous report, it has been done several simulations regarding thrust and flow efficiency in the duct. This is the foundation for the design of the ducts. The duct fan solution is supposed to be mounted on the DJI Flame wheel F450 quadrotor kit, and will therefor add significant mass to the quadrotor. Even though Balakrishnan has done work regarding saving weight, it is possible to reduce it more. This will be the main purpose of our thesis, since increased mass is highly undesirable on a quadrotor. The material chosen by Balakrishnan for his duct fan solution is the thermoplastic PA612-GF30 (Polyamide – Nylon). This is also the material used on the structure of the quadrotor DJI Flame wheel F450. In addition to the duct fan solution, the concept contains a top cover in the same material, which will protect the rotors from objects entering the rotors from above.

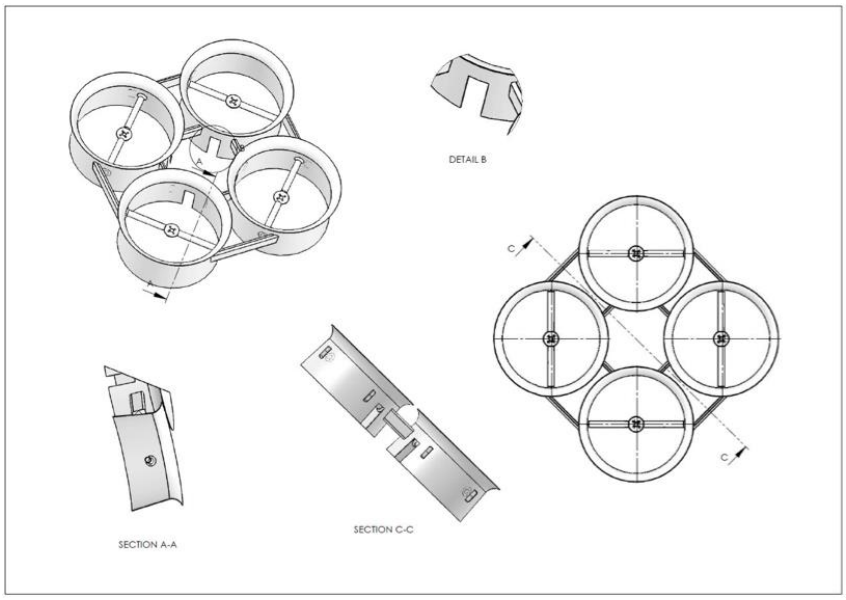

Figure 1. Duct fan solution [1].

Tests done using thrust measuring devices show nearly 40% improvement in thrust over an un-ducted quadrotor. The resulting weight of the duct was about 1150g. When including the added weight to the quadrotor, the increase in thrust is about 10% compared to the un-ducted quadrotor [1]. These results are so significant that it is interesting to continue the work. It is assumed that the weight can be lowered even more if the duct fan is built into the quadrotor. The master thesis will therefore continue the work of Balakrishnan and the main goal will be to reduce the mass by integrating the duct to the quadrotor and looking into other possible materials.

1.2 Problem description

The master thesis will look into the possibility of integrating the outer structure of the quadrotor with ducted fan solution in order to save weight. Balakrishnan's solution combines shielding of the rotors with increased thrust. This thesis will aim to save weight while maintaining the increased thrust compared to a non-ducted quadrotor. The ducts should be designed modular since it is likely that damage only occur to one duct while the others remain intact. A top cover for the ducts should also be a part of the final design. The quadrotor used in Balakrishnan's thesis is the DJI Flame Wheel F450, it is therefore natural to continue with the same quadrotor for this thesis. Robustness, availability and price are additional design criteria which we aim to fulfill, but will not be a design requirement.

2 Design process

2.1 Customer and design requirements

The task has some restrictions in terms of design of the quadrotor. In order to be successful, there are a few requirements that need to be fulfilled. These are requirements set from the customer. The most important requirement is to keep the weight at a minimum and at the same time keep the thrust equal to the previous solution. This will be a minimum requirement since the new concept is supposed to be an improvement of the previous work. To keep the thrust properties equal to the previous solution the inside of the duct needs to be approximately equivalent to the previous solution. A possibility of changing one duct fan at the time is a requirement from the customer. The body of the quadrotor will have to be stiff. If the structure has lack of stiffness several problems can occur, but it will most likely result in poor flying characteristics. There will be done a test regarding stiffness on the existing arms of the DJI flame wheel f450 quadrotor. The stiffness of a possible new frame should have approximately the same values in order to have the desired stiffness.

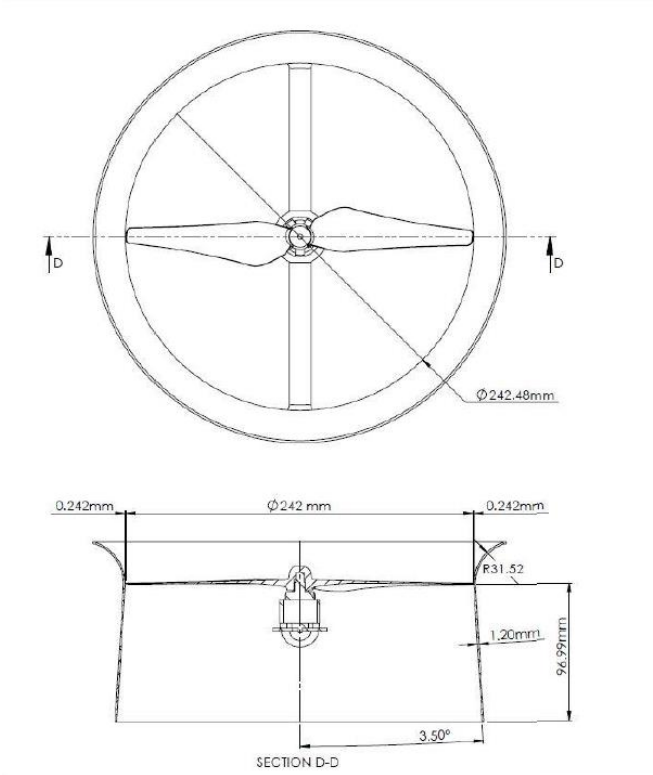

Figure 2. Balakrishnan's duct design [1].

Design specification bullet points:

- Lower weight
- Stiff frame, with the test results as a reference
- Modular ducts
- Inside geometry of ducts same as Balakrishnan’s design
- Low cost
- Robust

The two power distribution boards are PCB (Printed circuit boards) and contain important circuits for the electronic system of the quadrotor. It is therefore decided to keep the power distribution boards to avoid getting into subjects beyond our field of expertise.

2.1.1 Stiffness test

There will be done a stiffness test on one of the arms from the FJI flame wheel f450. This is done in order to generate specific data on the mechanical properties of the existing arms. It is important that the new solution will have approximately the same values as the existing arms in order to maintain the flying characteristics. When designing a new concept for the duct fan solution we need to take in consideration that the arms needs to be as stiff as the existing frame, analysis and test will be done as comprehensive as possible in order to verify the stiffness of the frame.

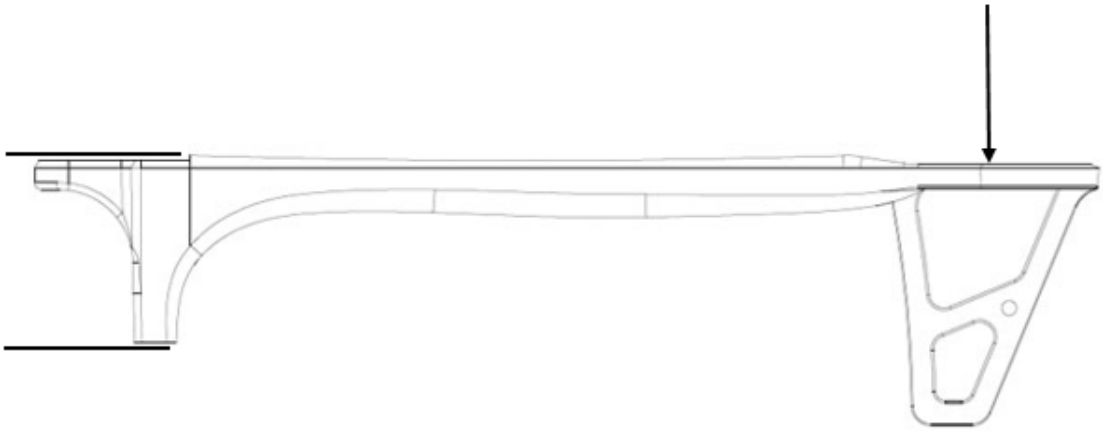

Figure 3. Stiffness test, deflection [2].

Two plates with holes corresponding to the holes in the frame arms are constructed. The plates are fastened to the arm, this makes it easier to clamp the end and that way make the end fixed. To measure the deflection, we add loads of different values at the point where the motor is fastened, as shown in figure 2.

2.2 Generating concepts

The design requirements are not strictly defined to a certain solution, so there is a high degree of freedom on how to solve the problem. This has led to several different concepts that vary vastly in design, but satisfy the requirements. Several methods have been used to select the most optimal design with regards to satisfy the requirements and available production methods and materials.

As mentioned in the design specification, the solution must be lightweight, modular and robust. Through brainstorming and discussion, five concepts were developed.

a) Drone arms integrated in the duct
b) Shorter custom arms, duct attached to arm
c) Custom frame attached to drone, duct attached to frame
d) Monocoque of a light material
e) Ducts made of a very lightweight material attached to a stiff and robust ring on the drone arms

Concept a), b) and c) are developed especially with 3D printing as a production method in mind. This is readily available on the UiT campus, and would be easy and close by if the dronelab need more parts in the future. Other production methods are also possible, but 3D printing was examined first. The idea of these three concepts is to shorten the arm on the drone, thus reducing the mass. However, it will lead to a challenge in mounting the engine. Since the engine is mounted to the drone arm in the original design, a shorter arm requires the engine to be mounted directly to the duct. Testing and analysis is required to find out if the duct is strong enough to support the added load of directly supporting the engine.

Figure 4. Concept A, B and C.

Concept d) would forego arms all together, instead supporting the duct and engines in a monocoque body of a lightweight material. After discussion and evaluation, it was deemed not modular enough to fulfil the customers wishes.

Concept e) would have a robust ring attached to the drone arms which would support the ducts made of a lightweight material such as Styrofoam or something similar. In the original design, most of the mass was in the ducts themselves, so by reducing this mass a large percentage of the total mass would be reduced. The duct will not be as robust as with a plastic material, but the ring will provide some protection against collision, and the foam material will absorb a lot of forces. If it breaks it will be easy and cost efficient to replace.

Weighted objectives

A – Lighter than original design

B – Modular

C – Robust

D – Low cost

Table 1. Objectives are weighted from 0 to 1.

Objectives	A	B	C	D	Total
A	-	0,5	1	1	2,5
B	0,5	-	1	1	2,5
C	0	0	-	1	1
D	0	0	0	-	0

Going along the rows, 1 means that objective A is more important than objective B. 0 means less important. 0,5 means they are equally important. Rank order is then A=B>C>D. Lighter and modular are demands given by the customer, so they are both weighted equally. Robustness is less important, but more important than keeping the cost as low as possible. If it continually breaks due to a frail design, it can even result in added expenses over time due to repairs and change of parts.

Morphological chart

Table 2. Overview of chosen concepts and features.

		Concepts					
Features		1	2	3	4	5	6
1	Attachement duct	Attached to original arms	Integrated in custom arm, duct not removable	Attached to custom arm, engine attached to duct	Custom frame mounted to drone, ducts mounted on frame	Monocoque of a light material	Superlight duct attached to a robust ring
2	Top cover	Balakrishnan's design	Wire mesh	Open	-	-	-
3	Custom arm	Sandwich construction	Milled aluminum	Injection molded plastic	3D printed plastic	-	-

The green line shows the concepts that was chosen. On the custom arm feature, the original arm was chosen, so the green line ends up on a blank box.

Evaluation matrix

Table 3. Evaluation of concepts.

	Concepts				
Selection criteria	A Duct with integrated arm	B Custom arm short	C Custom frame	D Monocoque design	E Super light duct
Lightweight	+	+	+	+	+
Modular	+	+	+	0	+
Robust	0	0	0	+	0
Production method	0	0	0	0	+
Sum +'s	2	2	2	2	3
Sum 0's	2	2	2	2	1
Sum -'s	0	0	0	0	0
Net score	2	2	2	2	3
Rank	2	3	4	5	1

The evaluation matrix compare the concepts to Balakrishnan's original design with regards to the design requirements and production method. [2]

2.3 Rapid prototyping

The requirements set from the customer does not say anything about production or material, which means we are free to choose the best material regardless of production method. Even though, it feels natural to consider a 3D printing design because of its advantages in manufacturing and the access to 3D printers at UiT. An equivalent solution could be made lighter and stiffer with another material, but when having a 3D printer available it is natural to consider a 3D printed solution as an alternative. When generating alternatives for 3D printing, there was a few limitations. The main limitation is the size of the 3D printer at UiT. We have access to a 290x290cm 3D printer. This means that it is not possible to 3D print the whole duct fan solution of Balakrishnan. It is also hard to calculate the mechanical properties of a 3D printed constructions because of the material which is constructed in layers and therefor has different properties in various directions. It will be done tests regarding stiffness on the final 3D printing solution to see if it is realistic to use it. The results will be compared with results from the stiffness test of the DJI flame wheel f450 arms.

After a design process, a few alternatives were generated. Throughout the process we were assisted from one of the persons with experience in 3D printing at the university. Together a concept was selected and printed in order to investigate the possibility of using a 3D printed solution as an alternative.

Figure 5. Final 3D print design.

2.3.1 Specifications

The 3D printed solution is a modified version of the previous duct design. It is added a structure to fix the duct to the power distribution boards directly. This is a solution with a shortened custom arm as mentioned in chapter 2.2. In addition to the shortened arm attached to the duct the structure is reinforced with two arms pointing 45 degrees out from the normal arm. This can be seen on figure 5. The arms are designed in a framework in order to save weight. The crossbeam inside the duct has been slightly modified to be structurally stiffer. It used to be hollow, but in order to achieve desired stiffness it's been made solid. Also, the cross section of the beam has been slightly changed to avoid too much deflection. It has been modified from a circle to an ellipse with greater diameter in the up-down direction. The original arm has threads to bolt the PCB to the arm. Because of the challenges of making threads when 3D printing another solution had to be made. The solution to this is to use nuts instead of threads in the arm. Ideal one could have used one bolt through the whole arm with a nut on the bottom to fasten both PCBs, this is not possible because the holes on the top and bottom of the PCB are slightly offset. Therefor a solution with square nuts inside the construction is made, this will allow the PCBs to be fastened without affecting the structure significantly. This solution will however need different bolts than the original. The original quadrotor uses M2.5x5mm bolts, this design will require longer bolts, preferably M2.5x15mm [3].

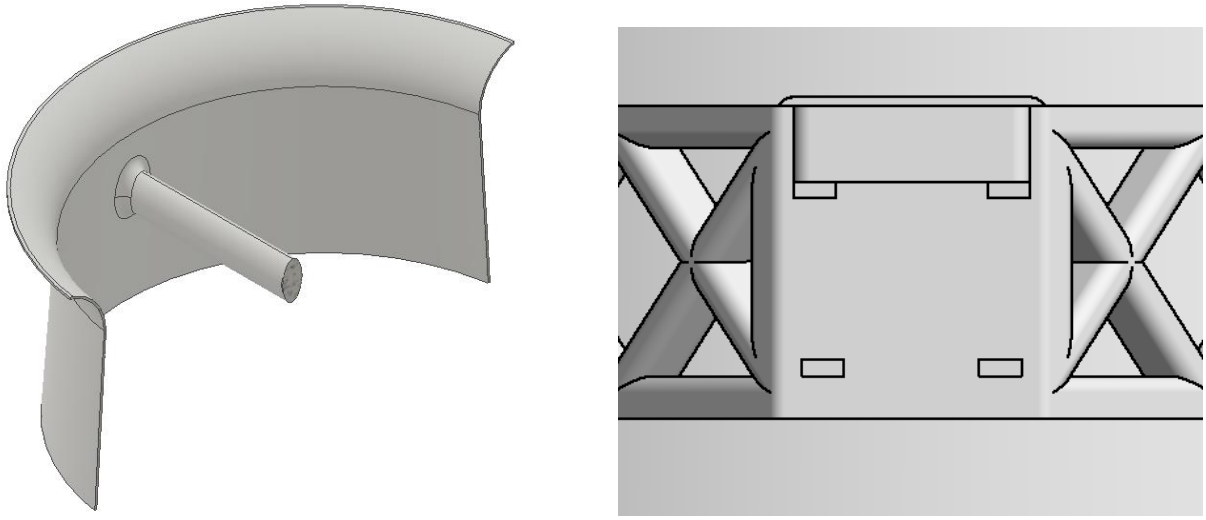

Figure 6. Cross section view and illustration of nut solution.

The material used in the 3D printed version is PLA plastic, it has a tensile strength between 30 and 40 MPa. Printing of the model were made with four layers as a maximum. This means that the 3D printer makes four layers with solid material and if a structure is thicker it compensates with making a honeycomb core. Practically for our model this means that the crossbeam is not solid, as we made it, but has a honeycomb structure inside. Total weight of the 3D printed version is 238.7g, this gives a total weigh for four ducts at 954.8g. This reduces the weight of the duct solution significantly. Balakrishnan's solution's mass is 1150g, when including the drone arms the total mass is 1366g not including top cover [1] [3]. In our design the original arms are not used so the total weight saving is 1366g – 954.8g+80g = 500.2g (including top cover). This is a weight saving of about a third of the previous solution for ducts, top cover and arms.

The main advantage of a 3D printed solution is that the production is relatively easy for the customer which have access to the 3D printer at UiT. There are some disadvantages with the design, primarily that it is considerably heavier than other solutions. The inaccuracy of the 3D print makes the nut solution not practical, the support structure from rapid prototyping blocks the hole and is difficult to remove. When evaluating concepts these pros and cons will have to be evaluated against each other. The customer will also give their opinion on what is weighted as more important.

2.3.2 Stiffness test of 3D printed solution and original arm

To investigate the stiffness of the 3D printed solution and the original DJI flame wheel F450 arm a stiffness test was performed. The process is described in part 2.1.1. Weight loads of different sizes were added to where the rotor is mounted and then deflection was measured. Weight loads of 500g and 2500g were used. Different measuring methods was used to ensure that the results were right. Results from the test show that the 3D printed solution has approximately the same stiffness for loads applied at the rotors mounting place.

Table 4. Deflections from the stiffness test.

Weight load	Original arm (mm)	3D printed solution (mm)
Method 1, 500g	1.77	1.77
Method 2, 500g	1.68	1.68
Method 1, 2500g	8.65	8.67
Method 3, 2500g	12	11

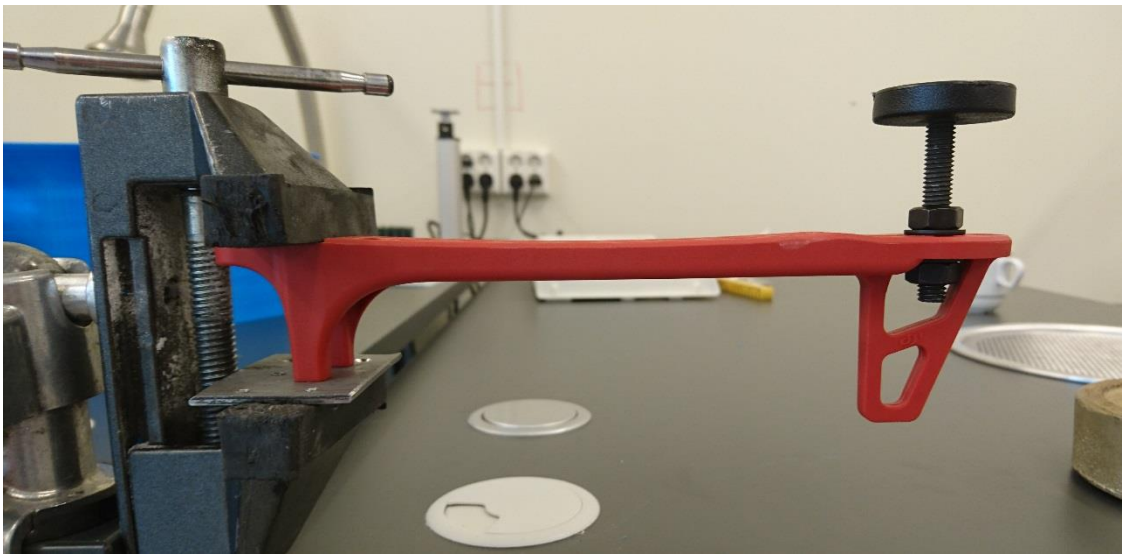

Figure 7. DJI Flame Wheel F450 arm.

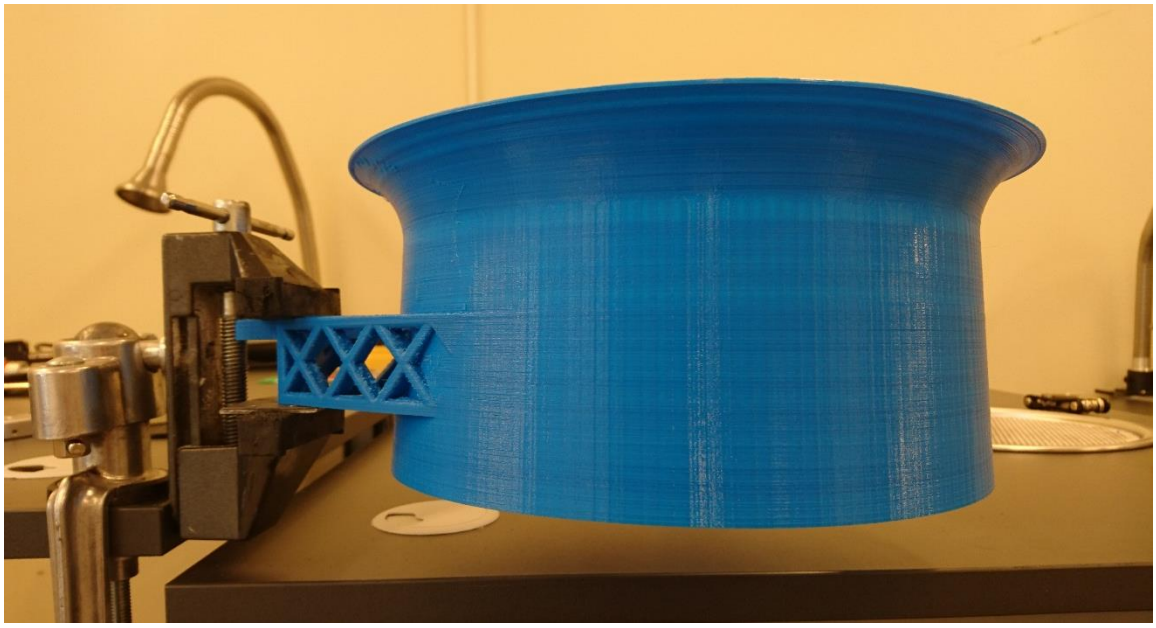

Figure 8. Duct with integrated arm, 3D printed.

3 Final design

After evaluation and meetings with the customer, concept E was chosen for the final design. Concept E had the highest potential for a large reduction in total mass, it is 100% modular, easily manufactured and the cheapest. A prototype of concept A was manufactured for testing as a viable solution. A full-scale model of the duct with an integrated arm was 3D printed, but unfortunately there was not enough of a reduction in mass compared to concept E. The production method was simple, but time consuming and the cost was about the same as Balakrishnan's original design. There would also be challenges related to the structural integrity of the integrated arm since the stabilizing rod would need to carry the entire load of the engine and related forces. Concept B and C suffered from the same drawbacks as concept A. Roughly the same cost, a very small reduction in mass and poorer structural integrity. Concept D was deemed not modular enough to fulfill the design requirements.

3.1 Early sketches

Early sketches of the final design.

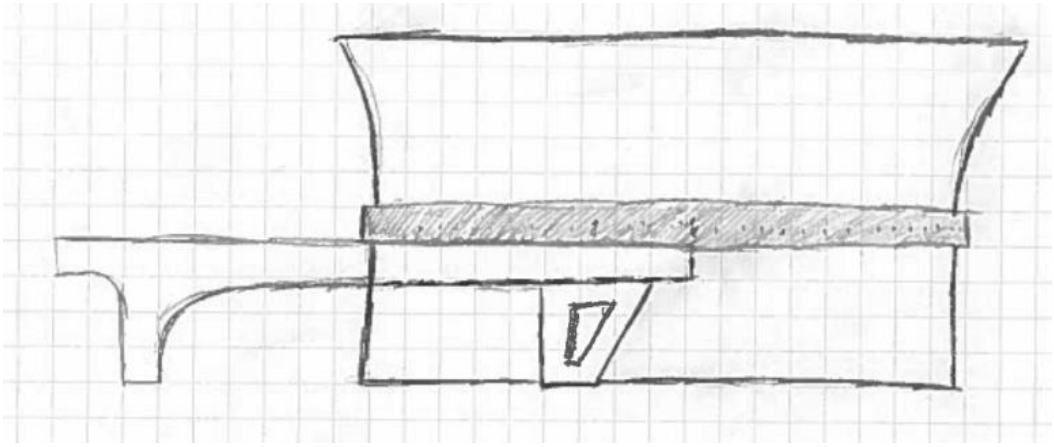

Figure 9. Profile of the duct with support ring and arm.

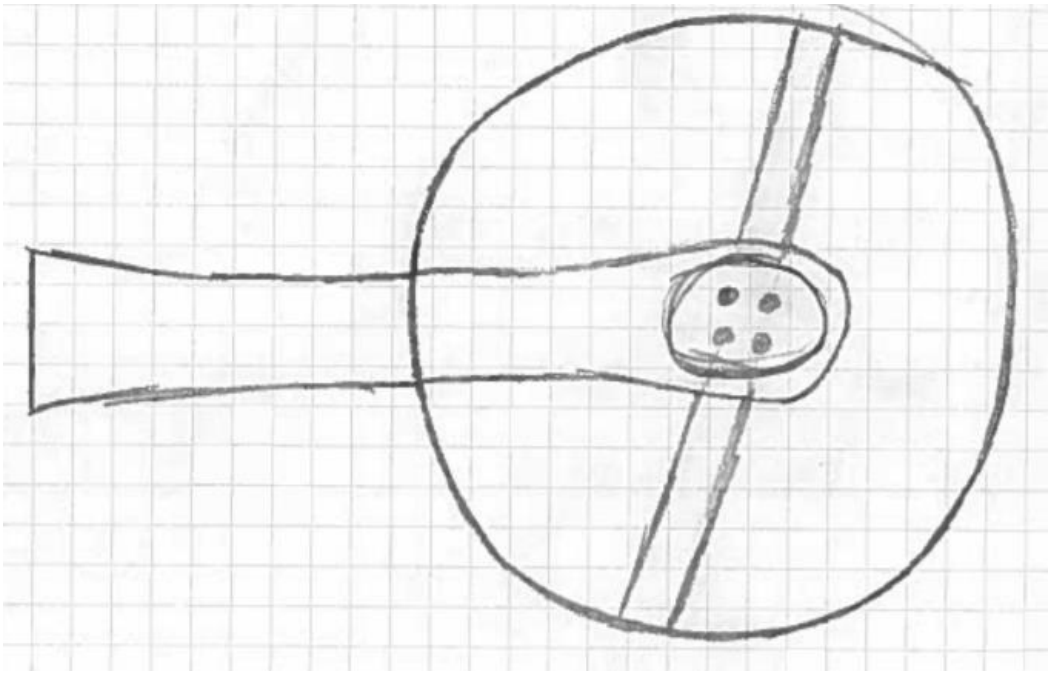

Figure 10. Top view of the duct.

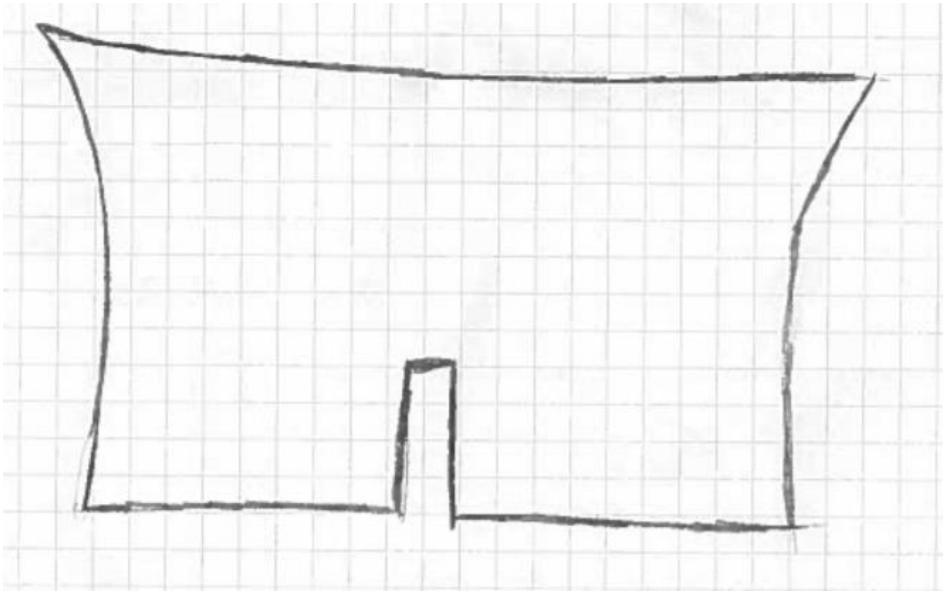

Figure 11. Profile of the duct showing the slit for the support ring.

3.2 Evaluation of different solutions

Two alternatives were discussed as possibilities for concept E. One where the original arm was kept, with a support ring mounted on top of the arm, and the duct placed inside the ring. The other would be a completely new custom arm with the support ring mounted on the edge of the arm, resulting in a shorter arm. The group decided to keep the original arm. This was the easiest solution, and would be a very robust and lightweight construction, keeping the stiffness of the original arm. The arm would carry most of the load compared to the shorter arm where the ring would carry most of the load.

Calculations were done with values from Balakrishnan's thrust testing regarding flight time of some of the different concepts. See table C-1 in appendix C for thrust values at different RPM, and external appendix F (preliminary work) about formulas regarding flight time.

Thrust (N)	**Power (W)**	**G**
(mass * G)/4	prop. const. * rpm^power factor/1000	9,81
Mass (kg)		
Balakrishnan	1,15	
Integrated duct	0,955	
Original drone	0,8	
Thrust Balakrishnan	4,78	
Thrust original	1,96	
Thrust integrated	4,30	
Thrust needed for test	3,9	
Flight time (min)	Battery capacity/Ampere used*60min	
Balakrishnan	12,78	
Original	18,5	
Integrated	18,5	
Test	28,29	

Propeller constant	**Power factor**
0,136	3,4
Power (W)	
Power bala	36,47
Power original	25,18
Power integrated	25,18
Power Test	16,48
Ampere (A)	I=P/V
Ampere Balakrishnan	13,14
Ampere original	9,07
Ampere integrated	9,07
Ampere test	5,94
Volt	**Battery capacity (Ah)**
11,1	2,8
RPM/1000	
Balakrishnan	5,179
Original	4,644
Integrated	4,644
Test	4,1

4100 rpm gives a thrust of 3,9N
The mass needed to reach this will then be

T*4/G	1,59	kg

Mass of the design must be less than 1590g-800g=790g

This gave a frame of reference for the total mass of the design. If the mass is kept under 790g, then only 3,9N of thrust is needed for the drone to hover. And this will result in a flight time of about 28min, which is a 10min improvement over the original design of the drone, and a 16min improvement over Balakrishnan's design [4].

3.3 3D model

The model consists of 3 parts, the support ring mounted on the drone arm, the duct placed inside the support ring, and the top cover placed on top of the duct. The support ring has a stabilizing rod with a mounting platform in the middle with holes corresponding to the mounting holes on the drone arm and engines. The mounting platform will be placed between the arm and engine. The duct is then mounted inside the ring. Slits on the sides are for the stabilizing rod, and the big slit in the front is for the drone arm. On the outside of the duct there is an edge for the support ring. This will help to secure the duct in place inside the ring, but will allow the duct to be removed. More pictures of individual parts can be

found in appendix A. Note that the wire thickness on the top cover is enlarged in the model pictures to properly showcase it. In reality the wire thickness will be much thinner.

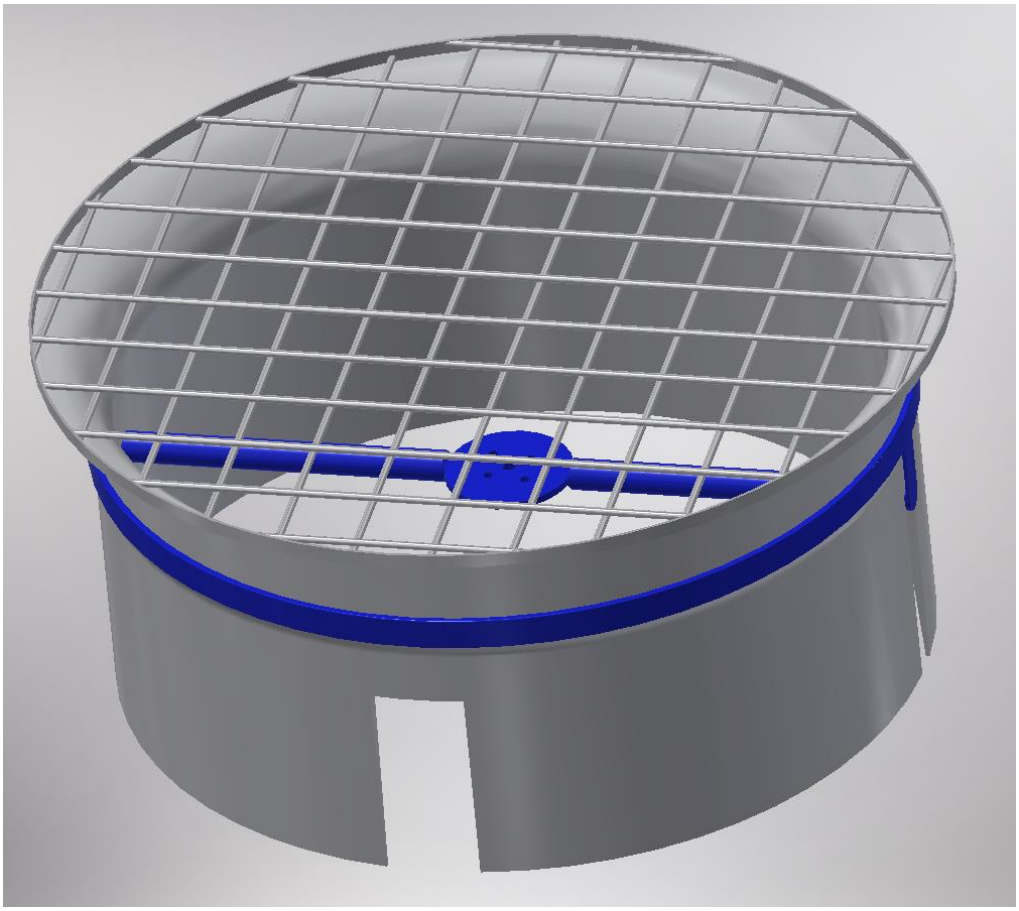

Figure 12. Final concept model.

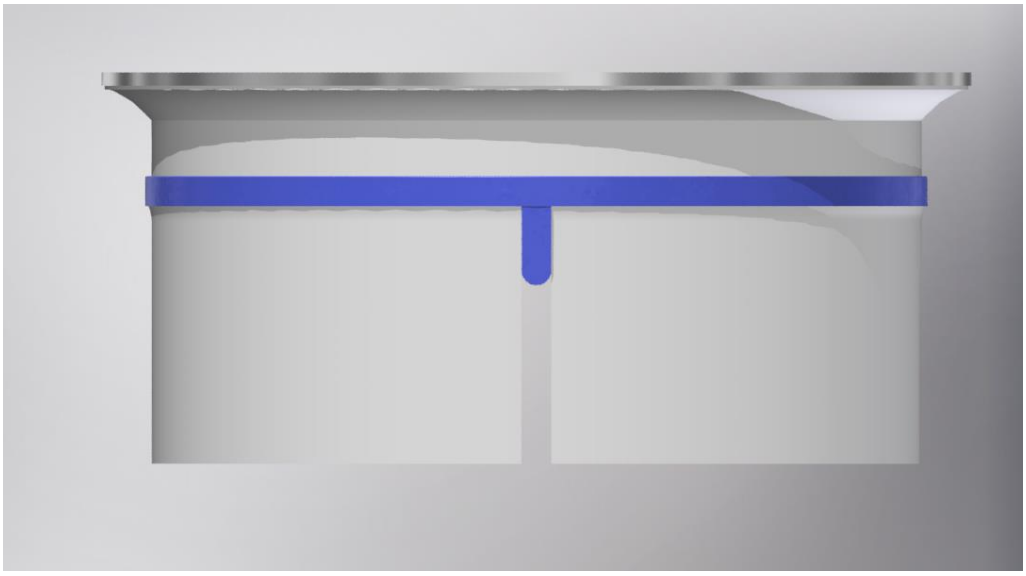

Figure 13. Side view of final concept.

4 Materials selection

4.1 Duct

For this analysis, the duct was regarded as a plate loaded with a bending force. It is simplified, but as Ashby says, "The simplification is rarely as critical as it may at first appear: the choice of material is determined primarily by the physical principles of the problem, not by details of geometry" [5].

Table 5. Materials selection criteria for duct.

Function:	Protect propeller and direct airflow
Constraints:	Radius R specified δ must not exceed the value from the test
Objective:	Minimize the mass m
Free variable:	Choice of material

The plates objective function is:

$$m = A\rho l \tag{1}$$

Where,

A = the area of the duct (m^2)

l = the length of the plate (m)

ρ = Density of the material (kg/m^3)

$$Area = b * t \tag{2}$$

$$Bending\ stiffness\ S = \frac{F}{\delta} \tag{3}$$

Where,

$b = width\ of\ the\ plate$

$t = thickness\ of\ the\ plate$

$F = force\ applied$

$\delta = Deflection\ of\ the\ plate\ due\ to\ the\ force$

Deflection of the plate is given by,

$$\delta = \frac{F * l^3}{C_1 * E * I} \tag{4}$$

Where,

$I = Second\ moment\ of\ inertia$

$E = Young's\ modulus$

$C_1 = A\ constant\ that\ depends\ on\ the\ distribution\ of\ loads$

Inserting this into bending stiffness,

$$S = \frac{F}{\frac{F * l^3}{C_1 * E * I}}$$

$$S = \frac{C_1 * E * I}{l^3}$$

$$I = \frac{bt^3}{12}$$

Inserting I into bending stiffness,

$$S = \frac{C_1 * E * (\frac{bt^3}{12})}{l^3}$$

$$S = \frac{C_1 * E * b * t^3}{l^3 * 12}$$

$$S = \frac{C_1 * E * b}{12}\left(\frac{t^3}{l^3}\right)$$

$$\frac{t}{l} = \left(\frac{12 * S}{C_1 * E * b}\right)^{\frac{1}{3}}$$

$$t = \left(\frac{12 * S}{C_1 * E * b}\right)^{\frac{1}{3}} * l \tag{5}$$

Inserting (5) into mass eqation,

$$m = btl\rho$$

$$m = b * \left(\frac{12*S}{C_1*E*b}\right)^{\frac{1}{3}} * l^2 * \rho$$

$$m = \left(\frac{12 * S}{C_1 * b}\right)^{\frac{1}{3}} * (bl)^2 * \left(\frac{\rho}{E^{\frac{1}{3}}}\right) \tag{6}$$

In equation (6),

$\left(\frac{12*S}{C_1*b}\right)^{\frac{1}{3}}$ is the functional constraint,

$(bl)^2$ is the geometric constraint,

$\left(\frac{\rho}{E^{\frac{1}{3}}}\right)$ is the material properties,

Where S,l,b and C_1 is specified. Material properties are left as a variable. This value is to be maximized, so it must be inverted to,

$$M_1 = \left(\frac{E^{\frac{1}{3}}}{\rho}\right)$$

Selecting the slope used in CES:

$$\frac{E^{\frac{1}{3}}}{\rho} = C$$

$$\frac{1}{3}logE - log\rho = logC$$

$$logE = 3logC + 3log\rho$$

$$y = 3x + constant$$

The resulting slope is 3 in CES with Young's modulus E on the y-axis and density ρ on the x-axis.

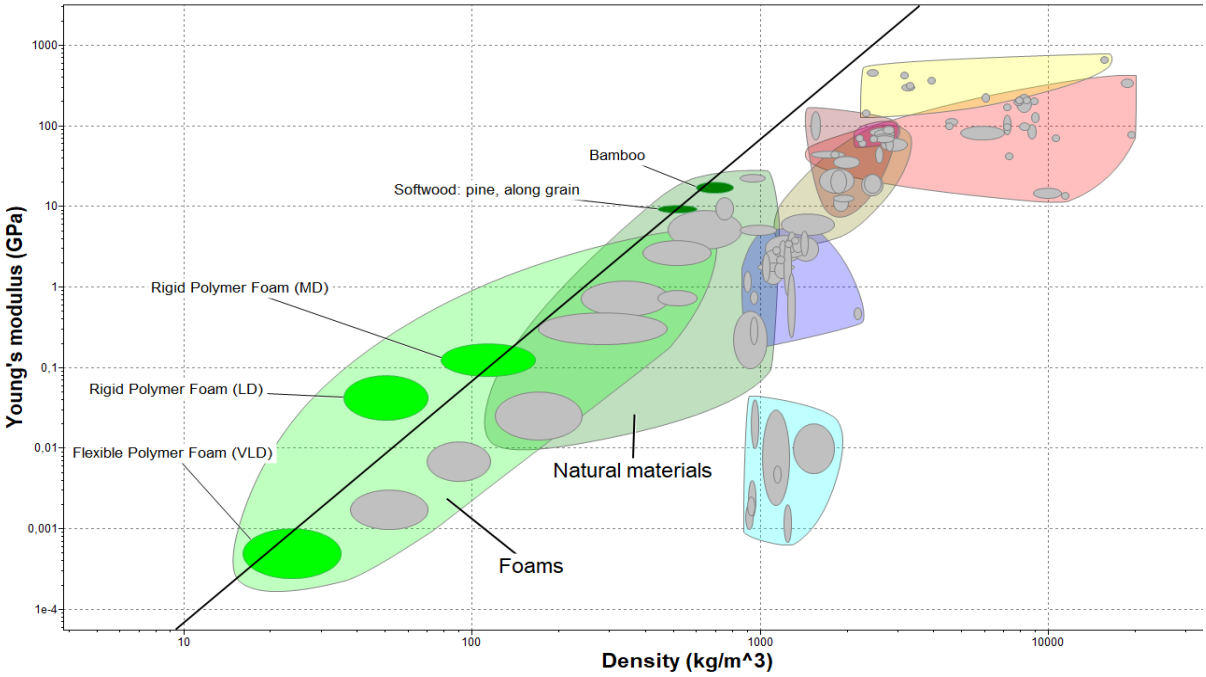

Figure 14. E- ρ chart showing the optimal materials for a low mass stiff duct.

Plotting the requirements into CES produced 5 possible materials.

Table 6. Densities of the materials given in CES.

Material	**Density (kg/m^3)**
Flexible Polymer foam (VLD)	16-35
Rigid Polymer Foam (LD)	36-70
Rigid Polymer foam (MD)	78-165
Softwood: Pine, along grain	440-600
Bamboo	600-800

As mentioned in chapter 3.2, the aim is to have a mass less than 790g. Using the volume of the design given in inventor, some calculations were done with the different densities of the materials from CES.

$V = 405088{,}066mm^3 = 0{,}000405m^3$

$m_1 = V\rho_1 = 0{,}000405m^3 * 16kg/m^3 = 0{,}00648kg = 6{,}5g$

$m_2 = V\rho_2 = 0{,}000405 * 36kg/m^3 = 0{,}01458kg = 14{,}6g$

$m_3 = V\rho_3 = 0{,}000405 * 70kg/m^3 = 0{,}02835kg = 28{,}4g$

$m_4 = V\rho_4 = 0{,}000405 * 165kg/m^3 = 0{,}066825kg = 66{,}8g$

$m_5 = V\rho_5 = 0{,}000405 * 440kg/m^3 = 0{,}1782kg = 178{,}2g$

These calculations are for 1 duct, so with 4 it is a total of,

$m_1 = 26g$

$m_2 = 58{,}3g$

$m_3 = 113{,}4g$

$m_4 = 267{,}3g$

$m_5 = 712{,}8g$

This rules out everything above 440kg/m^3 since this mass is getting close to 790g, and the mass of the support ring and top cover is still to be added. This also gives some leeway to make changes to design if needed.

To help choose between the different materials, limits were added. A strong material would be best suited so that the duct would not buckle or deform under load and damage the propeller.

Flexible polymer foam has a very low Young's modulus (<0,001GPa), and is usually used for cushions, mattresses and shock absorption in packaging. As the name suggests, since it is flexible, it is not stiff enough to serve as the duct. Low density rigid polymer foam (RPF) is very lightweight and solid. It is commonly used for isolation in buildings. It would be possible to use it as a duct, but it is very fragile. Medium density RPF is very lightweight and has just enough structural integrity to serve as a modular lightweight duct. It is used for disposable thermally insulating cups, lightweight structural use and as the core in sandwich panels. High density RPF is too dense for this project, and will add too much mass the duct. Since the design is relying on the outer ring for protection and the duct is only directing the air, the duct can be allowed to be weaker. Medium density RPF is strong enough to direct air and lightweight enough for this design. It is easily manufactured and comes in all shapes and sizes. Liquid raw polymer materials are poured into a paper mold where it foams and takes the shape of the mold. It is then stored for a day to cure the foam and cool. After it is cured, the blocks can be cut into whatever shape needed [6].

4.2 Support ring

The ring will provide some shielding for the propeller and duct and is placed in propeller height on the outside of the duct so it can absorb forces that would otherwise hit the propeller in a crash or similar circumstances. It has the same requirements as the duct, except it needs to be stronger to support the duct and shield against external loads.

Table 7. Materials selection criteria for support ring.

Function	Support and protect the duct
Constraints	Inner radius r is specified Ring must not buckle Stabilizing rod must be stiff
Objective	Minimize mass
Free variable	Material

The first material index that was maximized was the same as for the duct.

$$M_1 = \left(\frac{E^{\frac{1}{3}}}{\rho}\right)$$

Another index was added, since the ring needed to withstand some forces and provide some protection. The index $M_1 = \left(\frac{\sigma_y{}^{\frac{1}{2}}}{\rho}\right)$ and $M_1 = (\frac{E^{\frac{1}{2}}}{C})$ was maximized as well. This did not reduce the amount of

possible materials enough, so a limit was added. Since the drone may be operated in inclement weather, it must suitable to operate in watery conditions. So, by adding a limit that fresh water must be acceptable, the list of material shortened to 3 types of polymers, and 6 types of wood materials.

- Bamboo
- Hardwood oak, across grain
- Hardwood oak, along grain
- Plywood
- Softwood: pine, along grain
- Softwood: pine, across grain
- Cellulose polymers (CA)
- Polyamides (Nylons, PA)
- Polylactide (PLA)

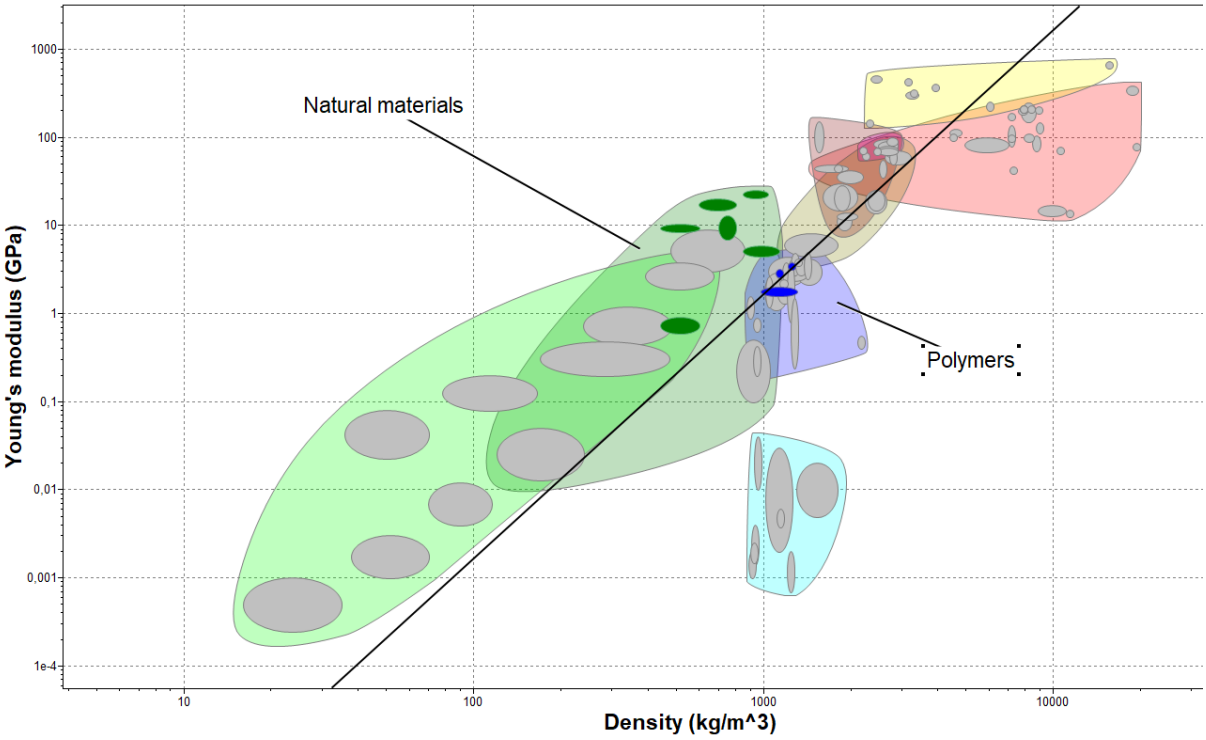

Figure 15. E- ρ chart showing the optimal materials for the support ring.

Looking at the remaining materials, the different types of wood has the lowest density. This would result in the lowest mass, but one of the polymers in the list was PLA. A lightweight, biodegradable polymer. The 3D printing machine available at the UiT campus in Narvik uses this material, so it would be quick and easy to manufacture. To manufacture the part in wood, one would need a lathe and cutting machines, and then glue together the ring and support rod. This makes the 3D printer an optimal choice. The part could be printed in one piece and be ready for use immediately.

4.3 Top cover

The top cover share many of the same requirements as the duct itself. It must be lightweight, robust, modular and not hinder the airflow through the duct. A very fine mesh is therefore to be avoided. Two concepts were evaluated.

Concept A:

Balakrishnan's ribbed top cover. Large holes as to not hinder airflow, low mass and cost. Fastened by pressing it over the edge of the duct. Fastening method not suited for this design when the duct is made of rigid polymer foam.

Figure 16. Top cover designed by Balakrishnan.

Concept B:

Wire mesh cover with a large mesh size. Fastened with an elastic band over the edge of the duct.

Balakrishnan's design was discarded in favor of a more suitable top cover. A wire mesh cover with a large mesh size and thin wires in aluminum fastened with an elastic band over the duct. The tapered shape of the duct will keep the elastic band down and the top cover in place on top of the duct. The size of the mesh will be small compared to the ribbed top cover, but will still be large enough as to not interfere with the airflow.

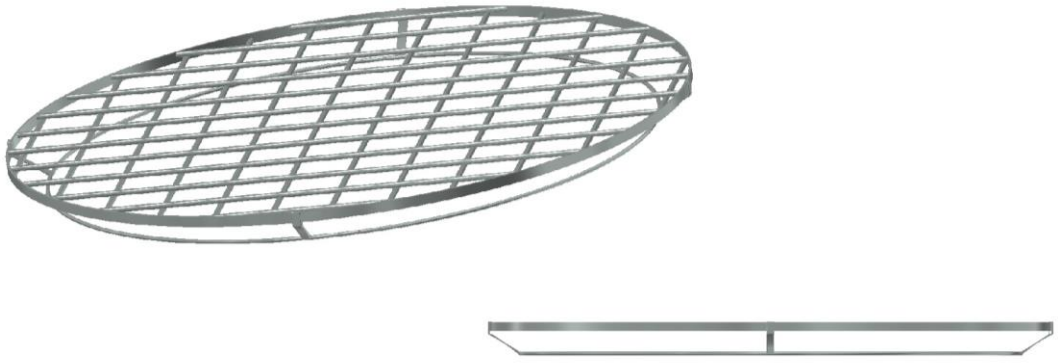

Figure 17. Wire mesh top cover.

5 Main results from numerical computations

The focus of the analysis will be on structural computations. Balakrishnan has already done computations regarding flow and thrust in his report and since there are only small changes on the inside of the duct there will not be done any computations or simulations related to this. The simulations will concentrate on structural strength of components in order to make the design as strong and stiff as preferred. The parts that will undergo numerical and analytical computations are the ring structure and the duct. There will be done structural simulations and analytical computations on the ring design and structural simulations on the duct. Results will be used to verify that the materials can withstand the forces and discover weaknesses in the structure. Numerical analysis is done with the Stress Analysis feature in Autodesk Inventor. Details about the simulation and the stress analysis setup can be found in appendix.

5.1 Analysis of ring

In order to run simulations it is necessary to find the maximal forces applied to ring. In normal circumstances this will be when the quadrotor accelerates as fast as possible based on Newton's second law of motion, $F = ma$. To simplify the simulation we look at forces acting in vertical direction. The quadrotor will be exposed to maximum forces when the thrust is at its highest. The maximum thrust for the quadrotor with ducted rotors is 9.1537N [1]. It is not stated how fast the Flame Wheel f450 can accelerate vertical so we do some calculations to achieve a number to work from.

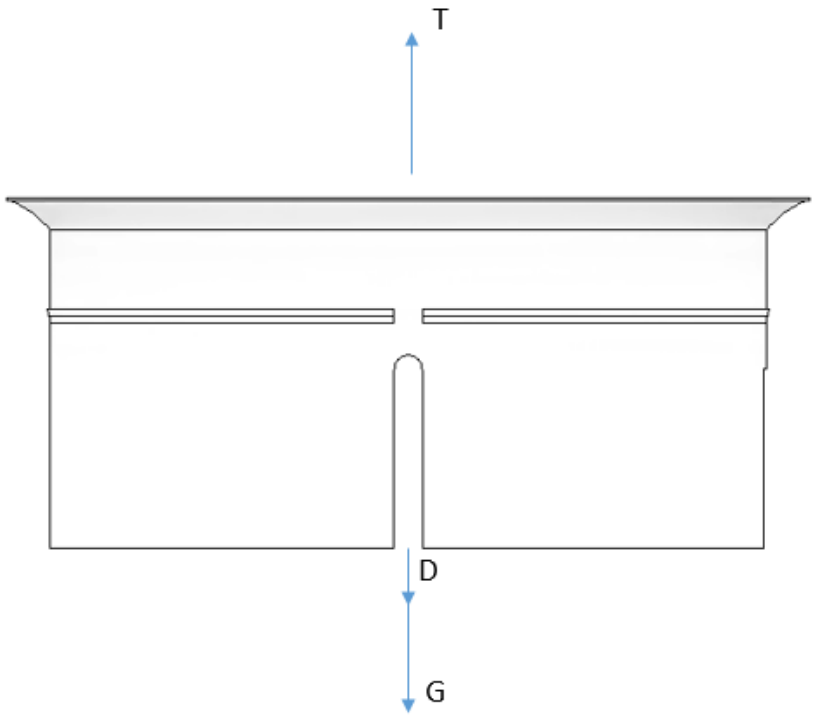

Figure 18. Forces acting on the ducted solution when accelerating vertically.

Figure 8 illustrates forces acting on the solution, T is the force generated from thrust, D is the drag from air resistance and G is the force from gravity. We know the maximal thrust generated by one rotor, this gives a total force of

$$T = 9.1537N \times 4 = 36.615\ N \tag{7}$$

The total weight of the drone, with the minimum takeoff weight of 800g [3] becomes

$$m = 1.33\ kg$$

from this we calculate G

$$G = 9.81\frac{m}{s^2} \times 1.33kg = 13.05N \tag{8}$$

We can calculate drag from the drag equation [7]

$$D = C_d \cdot \frac{\rho \cdot V^2}{2} \cdot A \tag{9}$$

were C_d is a drag coefficient that varies with the shape of the object. In our case we define the quadrotor as a flat plate and get a drag coefficient of 1.28 [8]. ρ is the density of air which is $1.225\ kg/m^3$ at 15^0C [9]. The drone's top vertical velocity is $6\frac{m}{s}$, we therefor set the velocity V to $6\frac{m}{s}$. We do an approximation on the surface of the quadrotor and define the area A as the area created from the edges of the quadrotor. With these values and approximations the drag equation (9) can be solved.

$$\mathrm{D} = 1.28 \cdot 1.225\frac{\mathrm{kg}}{\mathrm{m}^3} \cdot \left(6\frac{\mathrm{m}}{\mathrm{s}^2}\right) \cdot \frac{0.1318\ \mathrm{m}^2}{2} = 3.72\ \mathrm{N}$$

From equation 7, 8 and 9 the total force acting on the quadrotor then becomes

$$F = T - D - G = 36.615N - 13.05N - 3.72N = 19.845N$$

Use Newton's second law of motion and calculate the vertical acceleration of the quadrotor

$$F = ma = 19.845N$$

$$a = \frac{F}{m} = \frac{19.845N}{1.33kg} = 14.92\frac{m}{s^2} \tag{10}$$

From equation 10 we see that the acceleration the quadrotor will have is $14.92\frac{m}{s^2}$. We see clearly that this is not a realistic number, the acceleration is way too high to be realistic for this quadrotor. This is probably due to a very light takeoff weight. We have used Balakrishnan's results from thrust testing as a basis for the calculations and it is possible that these results are unrealistic when using the quadrotor properly. Even though the numbers are not realistic we use them for simulations, the numbers are too high and will give us a natural safety factor. The mass of the quadrotor is based on weight of the quadrotor, duct, ring and top cover at an early stage in the process. It is therefore possible that the final weight of the ducted solution will be slightly different from the mass used in the simulations.

5.1.1 Results from numeric simulations of ring

The simulation is done with a force defined as gravity and a force on the ring from the weight of the duct. Both of the forces are set up with the calculated acceleration. Inventor does not have PLA in its material library so the material properties are added manually. The material properties are obtained from the CES EduPack 2016 software. The ring is fixed under the engine mount and a force is added uniformly around the ring in addition to the gravity forces. Main results can be seen in figure 19 and 20.

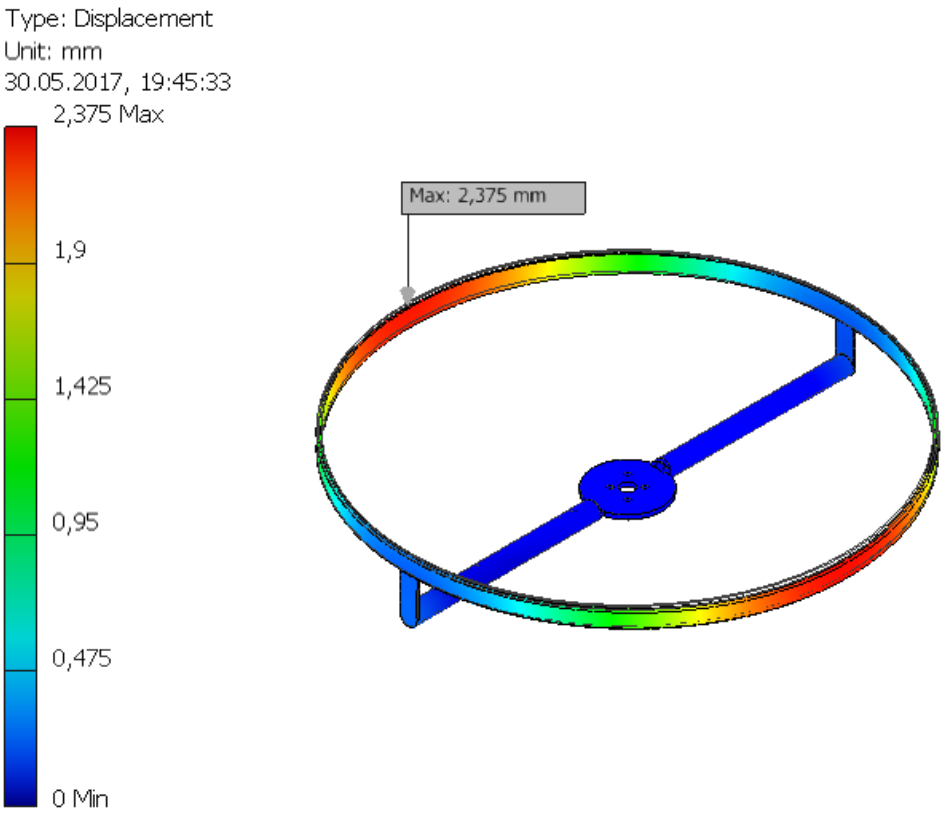

Figure 19. Displacement on ring with PLA plastic with forces from thrust, drag and gravity forces.

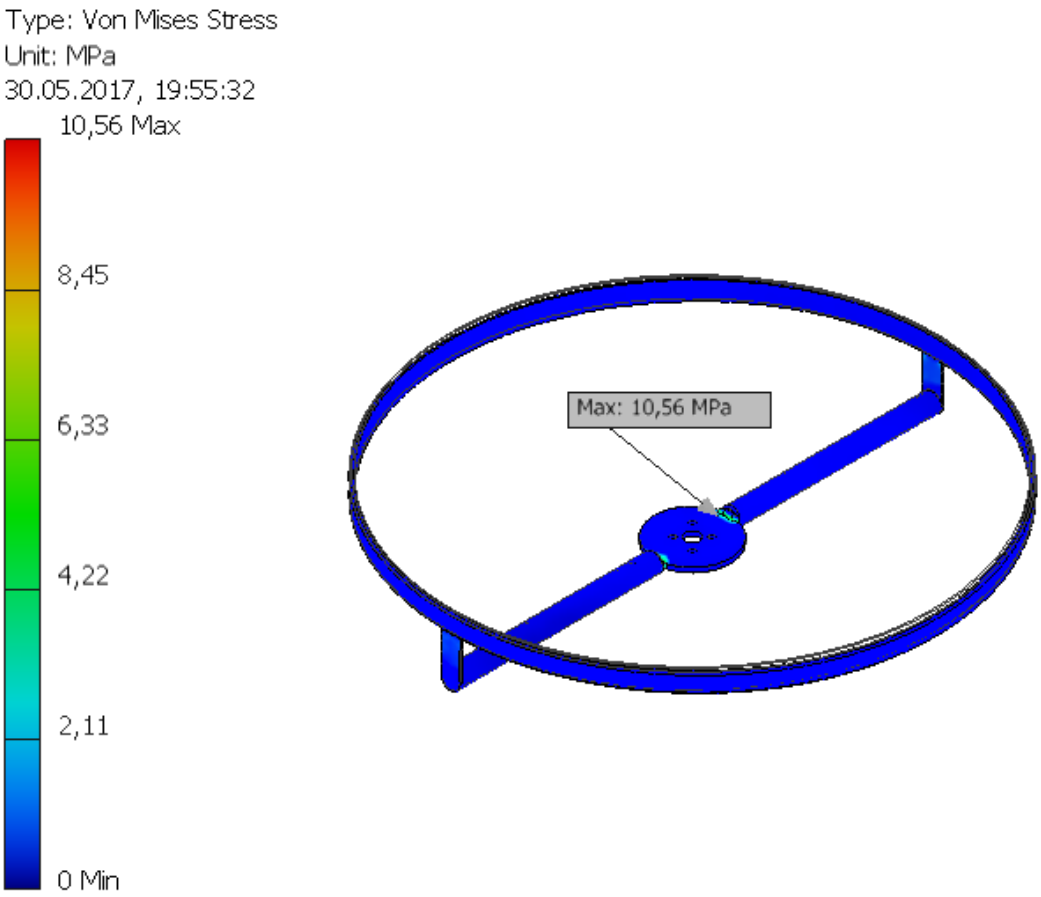

Figure 20. Von Mises Stress on ring made of PLA plastic.

Maximum deflection on the ring is 2.375mm. Maximum equivalent stress is 10.56 MPa. The results are satisfying regarding the mechanical properties of PLA. More details about the results can be found in appendix D.

5.1.2 Analytical calculation of ring

A calculation of deflection at the rods on the ring is done. Since the ring is symmetric we can look at one of the rods out from the motor mount at the time. The structure is simplified to a cantilever beam with a force at one end and fixed in the other end. The calculations are done to verify that the numerical simulations are correct. The beam deflection formula for cantilever beams are given in equation 11. Further the second moment of area for a thin walled cylinder is given in equation 12 [10] and the dimensions are shown in figure 21. To make the calculations as similar to the stress analysis in Inventor we use the same material properties as the numerical analysis. The calculations are done with the properties of PLA plastic. The force F corresponds to the mass of one duct.

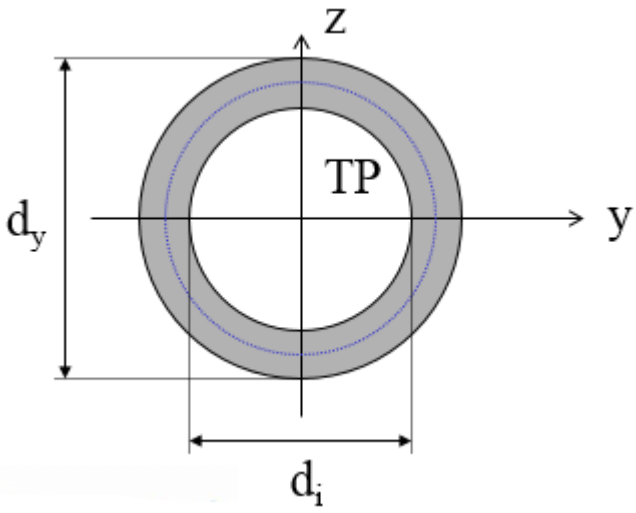

Figure 21. Cross section of rod [11].

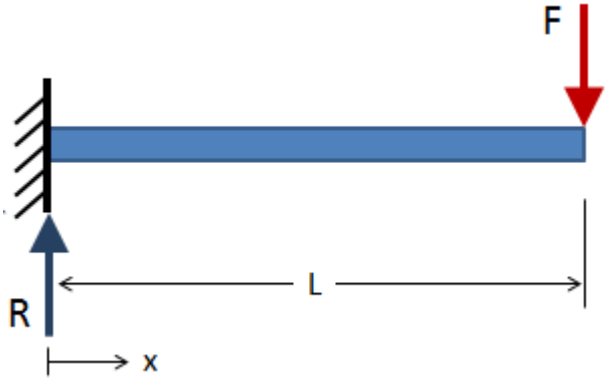

Figure 22. Cantilever beam [12].

$$u = \frac{FL^3}{3EI} \tag{11}$$

$$I = \frac{\pi}{64}({d_y}^4 - {d_i}^4) \tag{12}$$

$$F = 0.701N$$

$$E = 2.2 \cdot 10^9 Pa$$

$$d_y = 0.01m, \qquad d_i = 0.009m, \qquad L = 0.109m$$

$$u_{max.} = \frac{0.701 \cdot 0.109^3}{3 \cdot 2.2 \cdot 10^9 \cdot \frac{\pi}{64}(0.01^4 - 0.009)^4} = 8.15 \cdot 10^{-4}m$$

$$u_{max.} = 0.815mm$$

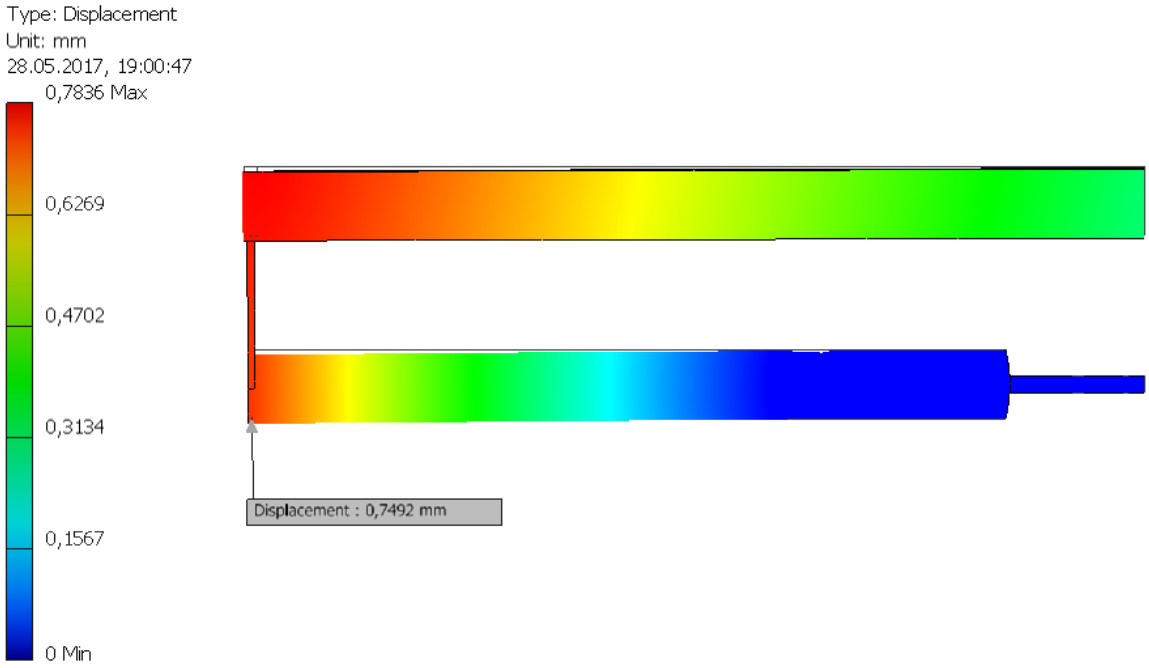

Figure 23. Deflection due to weight from duct.

The analytical computations gave 0.815mm as maximum deflection. This is almost the same as the numerical computations which gives a deflection of approximately 0.75mm at the end of the rod. This is shown in figure 18 were the ring is divided to make it like a cantilever beam. The rod is fixed at the right and a force is applied pointing downwards to make it as similar to the analytical computations. From this we can conclude that the simulations in Inventor are correct.

5.2 Analysis of duct

The duct will be affected by its own weight and additional forces created from thrust. It will also have to withstand the forces applied from the top cover. We do a numerical simulation for the duct isolated to generate limitations on material selection for the duct considering stress. The duct is fixed at the points were the rods from the ring meet the duct. A force corresponding to the weight of the top cover when accelerating is added at the contact point between the duct and the top cover. More details can be found in appendix D.

5.2.1 Results from numerical simulation of duct

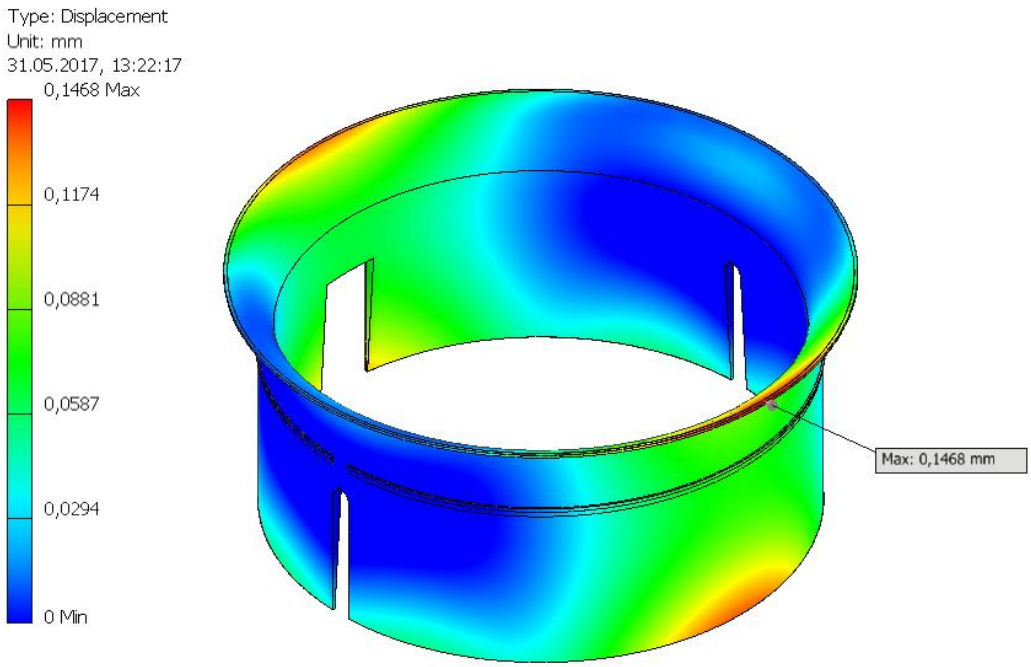

Figure 24. Displacement on the duct.

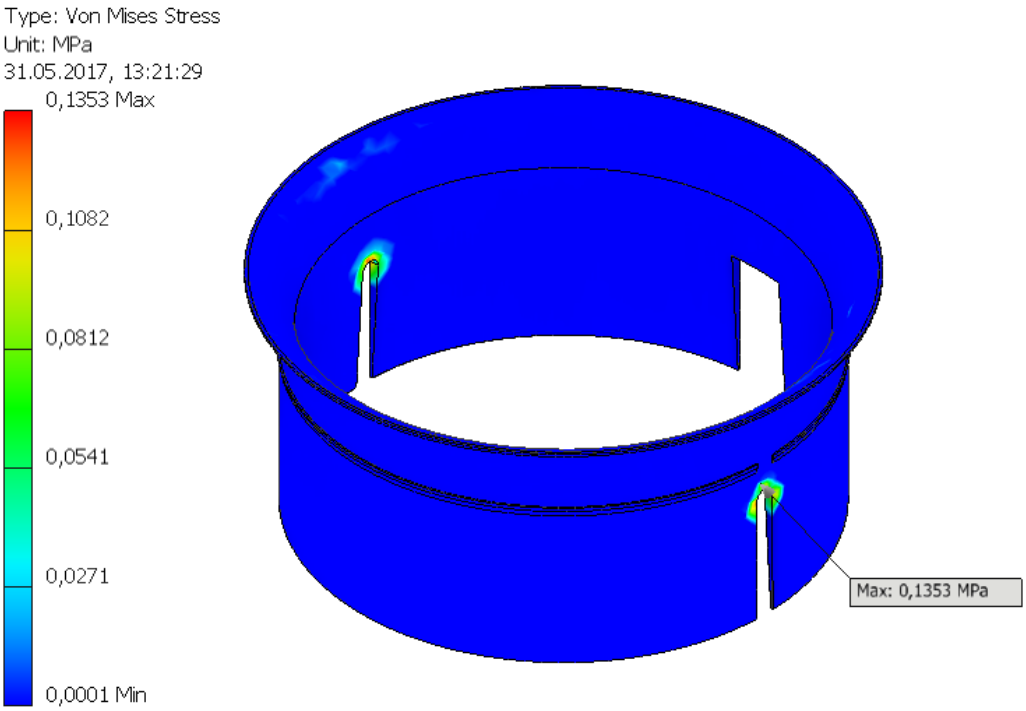

Figure 25. Von Mises stress on duct.

Maximum Von Mises equivalent stress is approximately 0.14 MPa. Maximum deflection is 0.15mm. The results are within the mechanical limits of rigid polymer foam. More detail can be found in appendix D.

5.3 Simulation of whole duct structure

The whole assembly is simulated with the acceleration calculated in section 5.1. It is fixed were the quadrotor arm is fastened. Inventor generates the contact between the different parts. More details about the simulation can be found in appendix D.

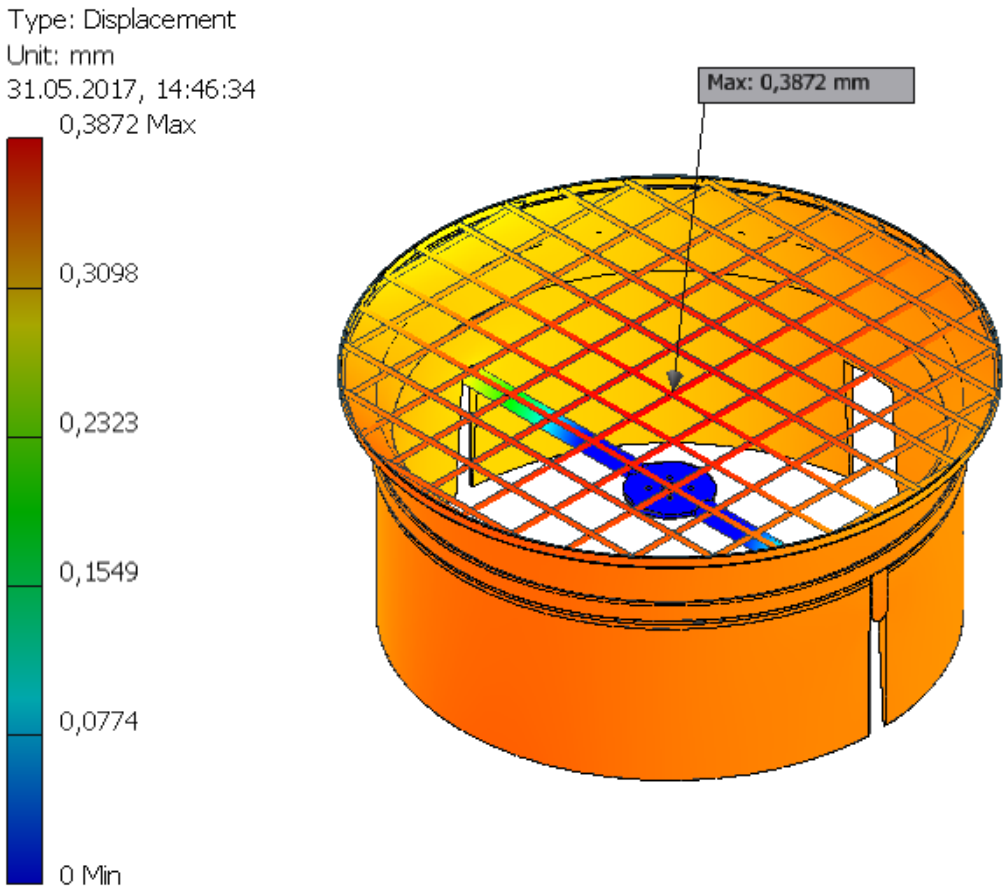

Figure 26. Displacement of ring, duct and top cover.

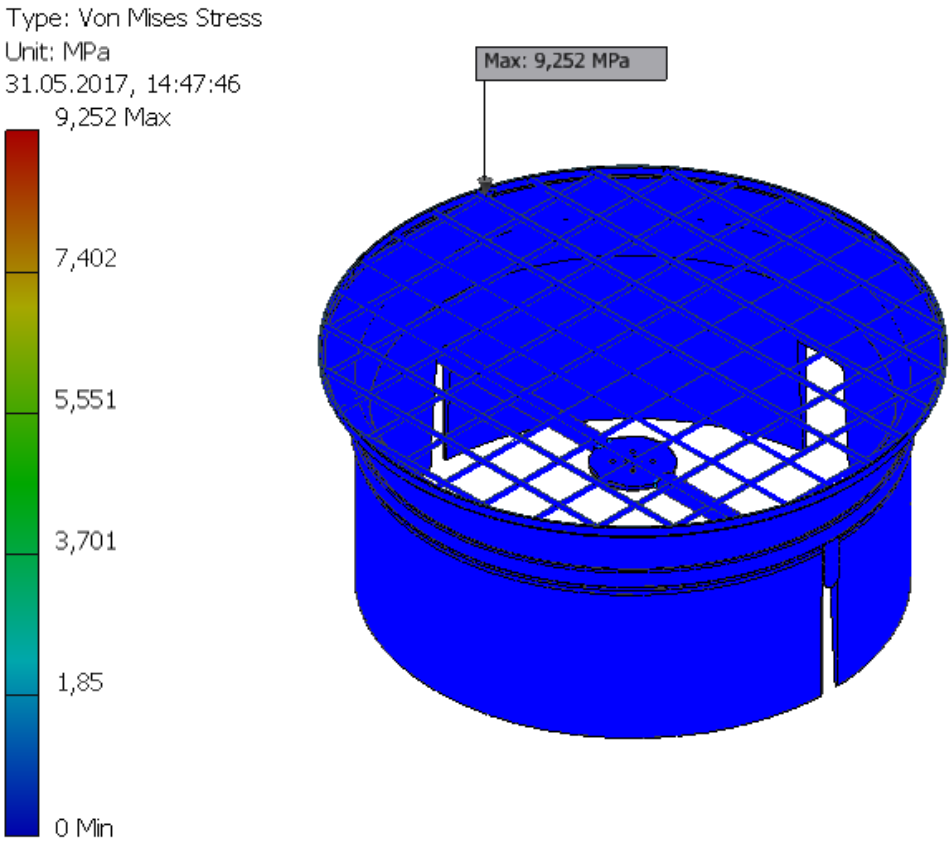

Figure 27. Von Mises stress on ring, duct and top cover.

Maximum Von Mises stress on the whole ring and duct solution is 9.252 MPa at the edge of the top cover. Maximum displacement is 0.9452mm located at the center of the top cover. Even though the displacement is almost 1mm it will not create any conflict with the rotors or anything else. The stress is within the limits. More details can be found in appendix D.

6 Results and discussion

The final design of the duct fan solution has significant reduction in weight compared to Balakrishnan's solution. We have come to a solution where the ducted fan is not integrated in the quadrotor structure. This is done because of various reasons, but mainly because in that way we keep the properties of the frame arm which is optimized for the quadrotor. Without any physical tests, it would be difficult to determine properties like the arms ability to transfer vibrations through the frame which could cause the quadrotor to vibrate while flying. This will most likely affect the flying characteristics. Our design includes three main parts, duct made of medium density RPF, a ring made of PLA and top cover in aluminum. In addition, an attachment solution for the top cover containing an elastic band that holds the top cover in place. This is illustrated in the CAD model. When discussing the possibility of saving weight, the idea of having a duct which was not a part of the supporting structure came up. This gave us the opportunity of using a very light material on the duct. The idea was that the duct only had the purpose of providing increased thrust, the propeller shielding should be done by a smaller structure which also held the duct in place. This became the ring structure. The top cover is designed as a wire mesh, this would offer better protection to the propeller than the previous solution. One of the design requirements were that the solution should be modular. In the final design the three main parts are all modular. The duct is most likely to be damaged as this is the most fragile part. The ring is more structurally solid and is made to protect the rotors, but if subjected to a more powerful impact the ring will most likely be damaged. It will take a greater force to damage the top cover so this part is not likely to be damaged.

The mass of the duct and ring are obtained from Inventor. The density of the material is manually entered due to inequality between properties in Inventor and CES and lack of the material in the Inventor material library. The mass of the top cover is obtained from a producer of wire mesh [13].

Mass	**Density**
$m_{duct} = 66.825g$	$\rho = 165kg/m^3$
$m_{ring} = 33g$	$\rho = 1240\text{kg/m}^3$
$m_{top\ cover} = 61.5g$	$\rho = 2700\text{kg/m}^3$

The total weight of the of the ducted fan structure will be

$$m = (m_{duct} + m_{ring} + m_{top\ cover}) \cdot 4$$

$$m = 267.3g + 132g + 246g = 645.3g$$

The rubber band add a small amount of weight so we round up the total mass to

$$m_{tot.} = 650g$$

In figure 28 and 29 the whole quadrotor is illustrated. The parts from the original quadrotor are obtained from Balakrishan's project.

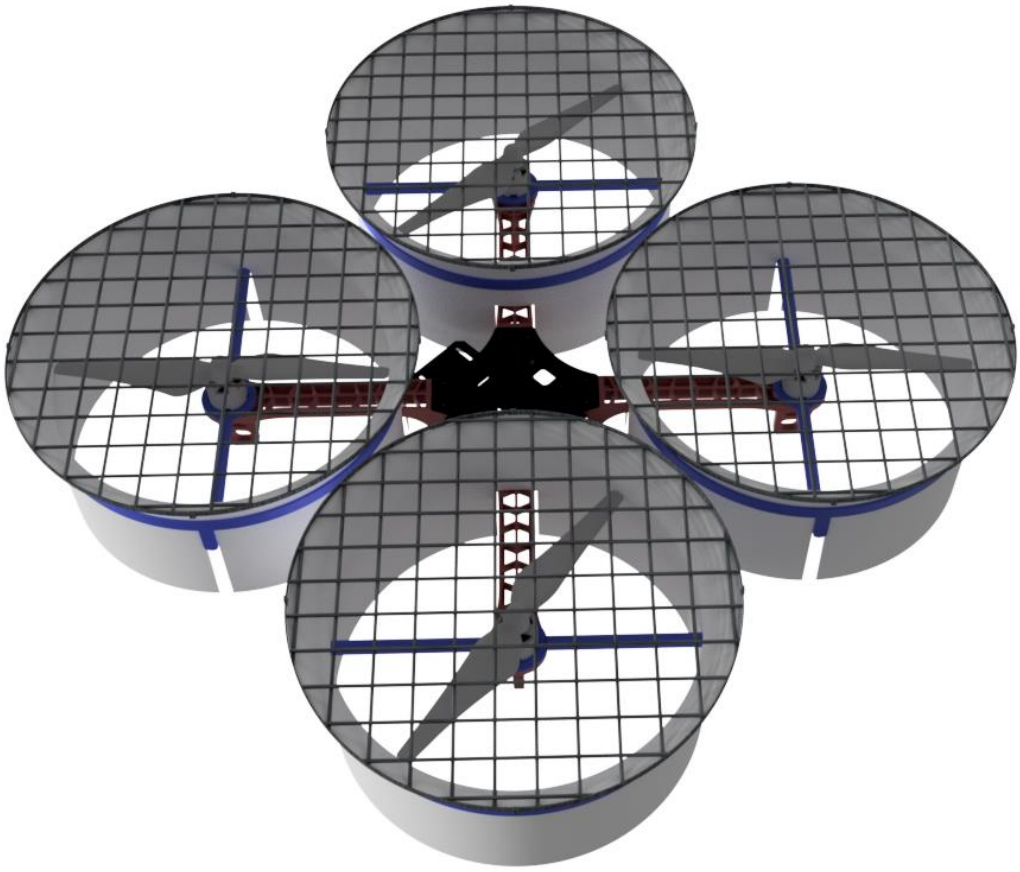

Figure 28. Final solution.

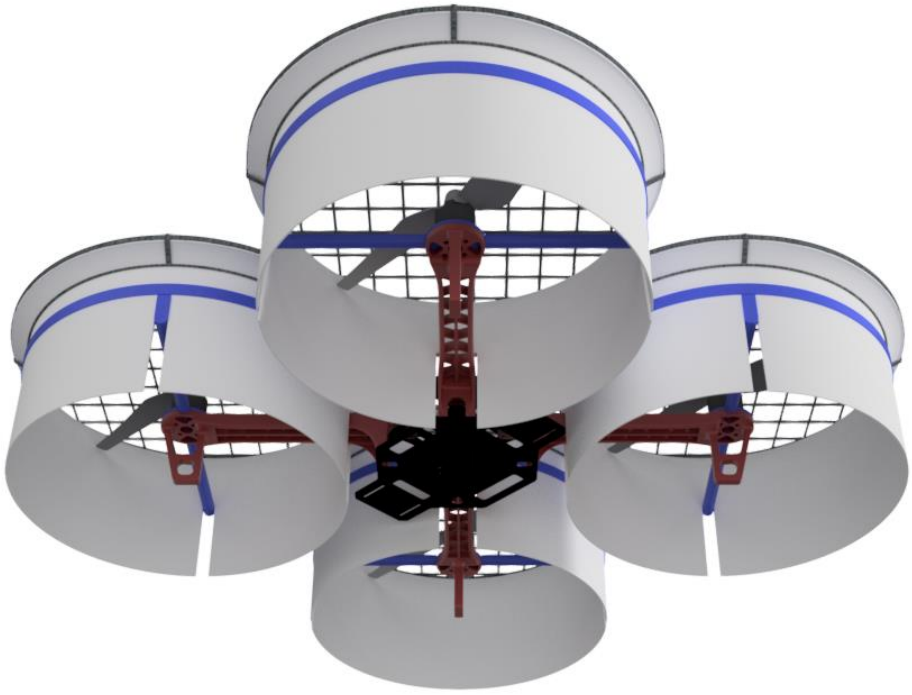

Figure 29.Final solution seen from underneath.

6.1 Prototype

The prototype was constructed by plates of Styrofoam glued together and a 3D printed support ring. The scale of the support ring is accurate, but the Styrofoam duct is thicker than the design due to the coarse nature of the Styrofoam making it difficult to cut into a thin walled duct. The prototype gives insight to the relative size and weight of the final product, and demonstrates how the modular aspect of the design works. No physical tests were conducted as the production method and material is not as described in this report. Note, in figure 31 the rotor is placed too low inside the duct.

Figure 30. Prototype in styrofoam.

Figure 31. Prototype with drone arm and rotor.

7 Conclusion

The goal for this project has been to reduce the mass of a ducted fanned shielding design for quadrotors without affecting the positive thrust performance from the ducts. The thesis continues the work of a previous master thesis written by Sethuram Balakrishnan and introduces a new design for his ducted fanned shielding design for the DJI flame wheel f450 quadrotor. A systematic design and material selection process together with simulations has resulted in a solution that reduces the mass significantly. A prototype for one of the rotors was constructed. During the preliminary work design requirements were compiled. As a result of the design process the following specifications were fulfilled.

- Lower weight.
- Stiff frame. As the frame arms are from the original quadrotor the arms have the desired stiffness.
- Modular ducts. All three main part in the design are modular.
- Inside geometry approximately the same as Balakrishnan's design.
- Low cost.

The total mass of the final design is 650g. This reduces the mas from Balakrishnans design with

$$1150g - 650g = 500g$$

For the ducted fan solution, this gives a percentage weight loss of

$$\frac{500g}{1150g} \cdot 100 = 43.5\%$$

7.1 Suggestions for future work

Due to a limited time frame available on this project, proper physical testing of the finished product was not conducted. A prototype of one duct and support ring was manufactured for visual purposes, but more testing is needed to verify if the finished product is acceptable. The duct especially could be analyzed more extensively, with more detailed physical analysis to verify if the construction is rigid enough to provide adequate protection of the propeller. A new flow analysis may also be needed to check if the surface roughness of the rigid polymer foam disturbs the airflow through the duct. Testing of the actual flight times, and comparing them to the projected flight times calculated in this rapport is also something that could be done in future work.

8 References

[1] S. Balakrishnan, "Duct fanned shielding design for quadrotors," UiT, Narvik, 2016.

[2] N. Cross, Engineering Design Methods, strategies for Product Design, Chichester: John Wiley & Sons Ltd, 2000.

[3] DJI, "FlameWheel 450 User Manual," DJI, 2015.

[4] J. Dickey, "quadcopterproject," 2011. [Online]. Available: https://quadcopterproject.wordpress.com/battery-and-flight-time/. [Accessed Januar 2017].

[5] M. F. Ashby, Materials Selection in Mechanical Design, Butterworth-Heinemann, 2005.

[6] C. Udumbasseri. [Online]. Available: https://www.slideshare.net/ChandranUdumbasseri1/manufacturing-polyurethane-foams. [Accessed 23 Mai 2017].

[7] J. Glenn, "NASA Glenn Research Center, The Drag Equation," 05 2015. [Online]. Available: https://www.grc.nasa.gov/www/k-12/airplane/drageq.html. [Accessed 16 05 2017].

[8] J. Glenn, "Nasa Glenn Research Center, Shape Effects on Drag," 2015. [Online]. Available: https://www.grc.nasa.gov/www/k-12/airplane/shaped.html. [Accessed 16 05 2017].

[9] "The Engineering ToolBox," [Online]. Available: http://www.engineeringtoolbox.com/air-density-specific-weight-d_600.html. [Accessed 18 05 2017].

[10] T. Schive, "Meccanica," [Online]. Available: http://meccanica.uit.no/fasthet/20t.html. [Accessed 24 May 2017].

[11] P. E. Thoresen, "iu.hio.no," 31 March 2004. [Online]. Available: http://www.iu.hio.no/~pererikt/Konstr/mekanikk-en/presentasjoner/leksjon-17.ppt. [Accessed 26 May 2017].

[12] Mechanicalc, "MechaniCalc," [Online]. Available: https://mechanicalc.com/reference/beam-analysis. [Accessed 28 May 2017].

[13] TWP, "twpinc.com," [Online]. Available: https://www.twpinc.com/wire-mesh-material/aluminum/aluminum-bird-mesh.

[14] P. E. Thoresen, "iu.hio.no," 02 May 2006. [Online]. Available: http://www.iu.hio.no/~pererikt/Konstr/mekanikk-en/presentasjoner/. [Accessed 25 May 2017].

Appendix

A. 3D models from Inventor

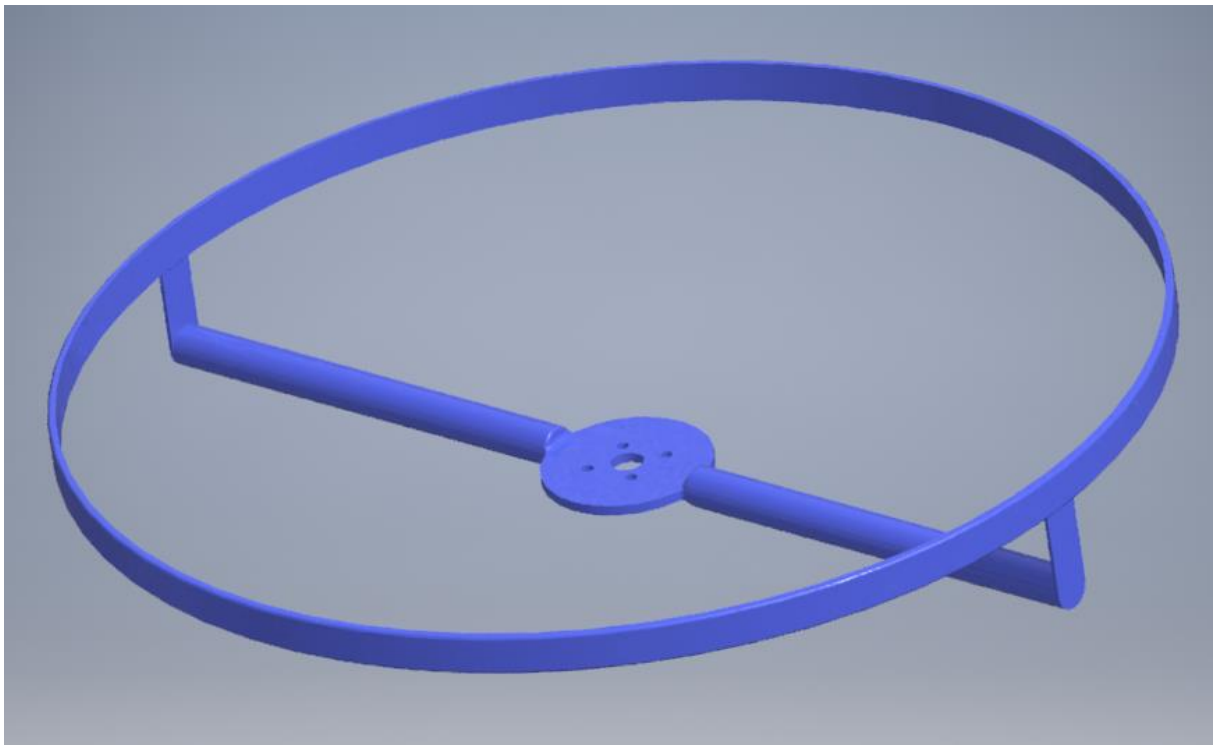

Figure A-1. ISO view of support ring.

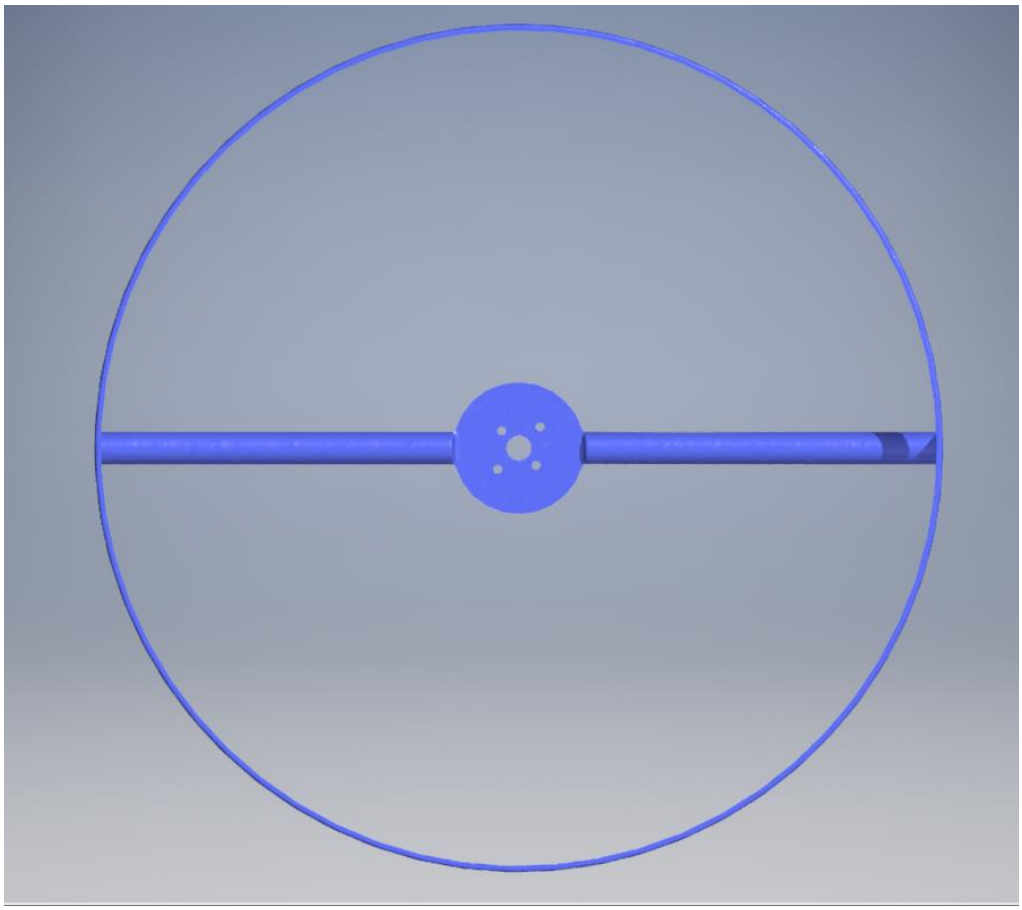

Figure A-2 Top view of support ring.

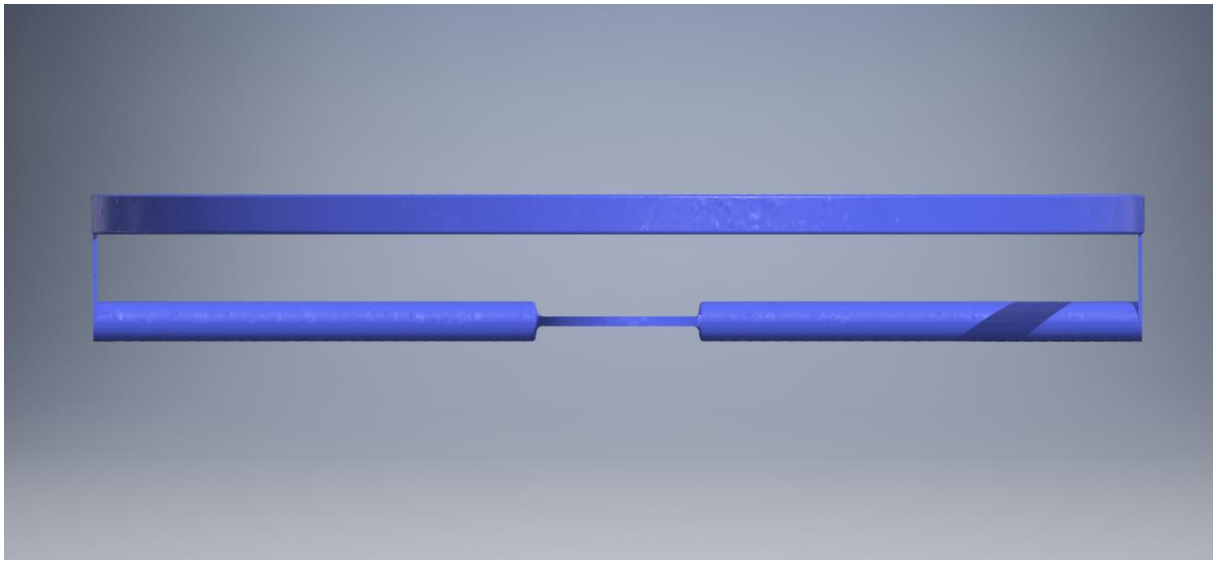

Figure A-3. Front view of support ring.

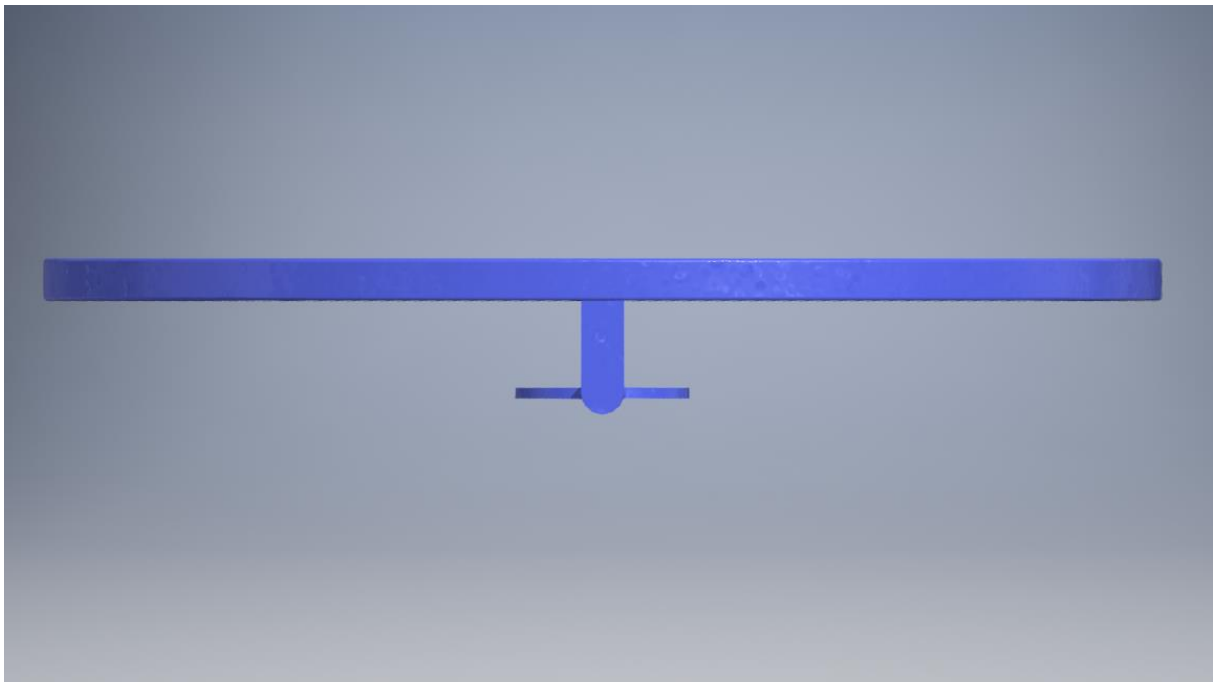

Figure A-4. Side view of support ring.

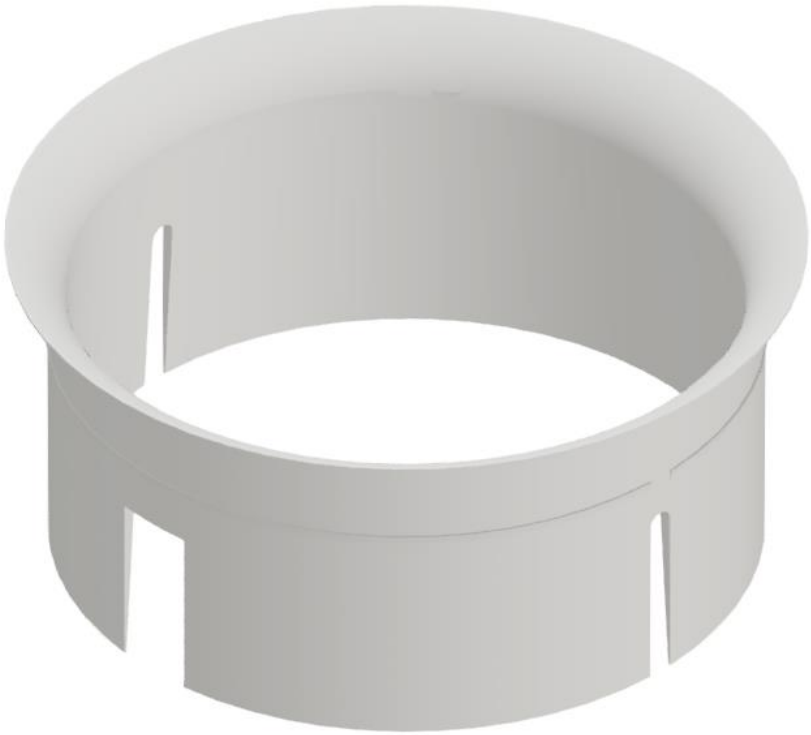

Figure A-5. ISO view of duct.

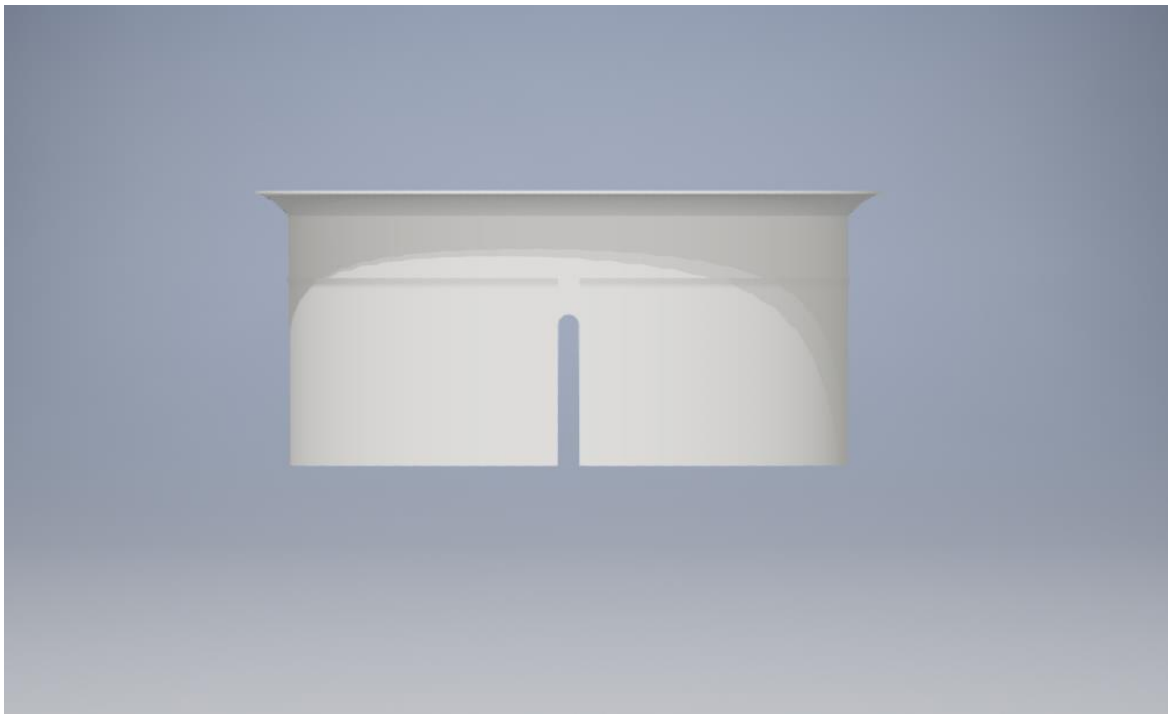

Figure A-6. Side view of duct.

B. 2D drawings

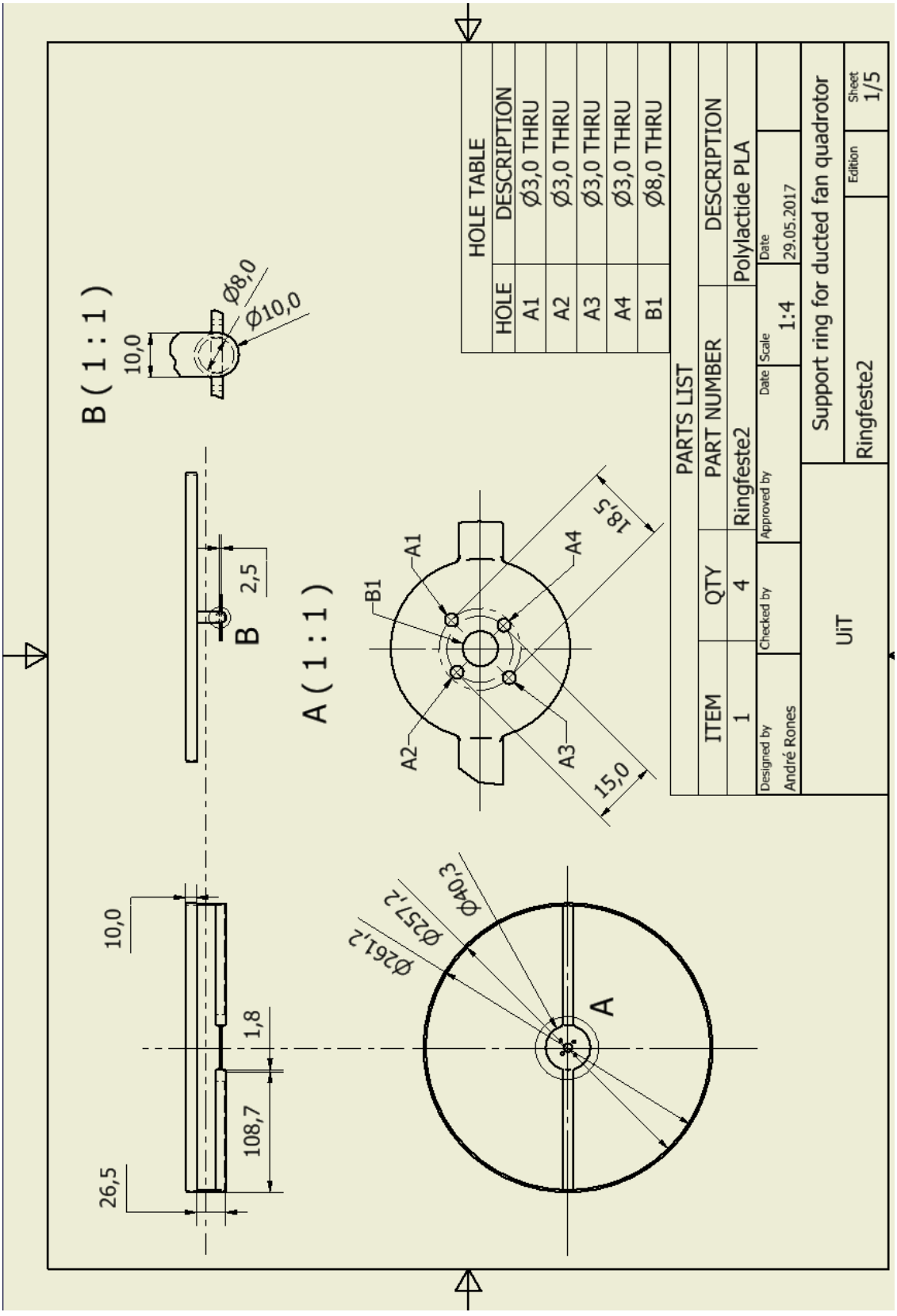

Figure B-1. 2D drawings of support ring.

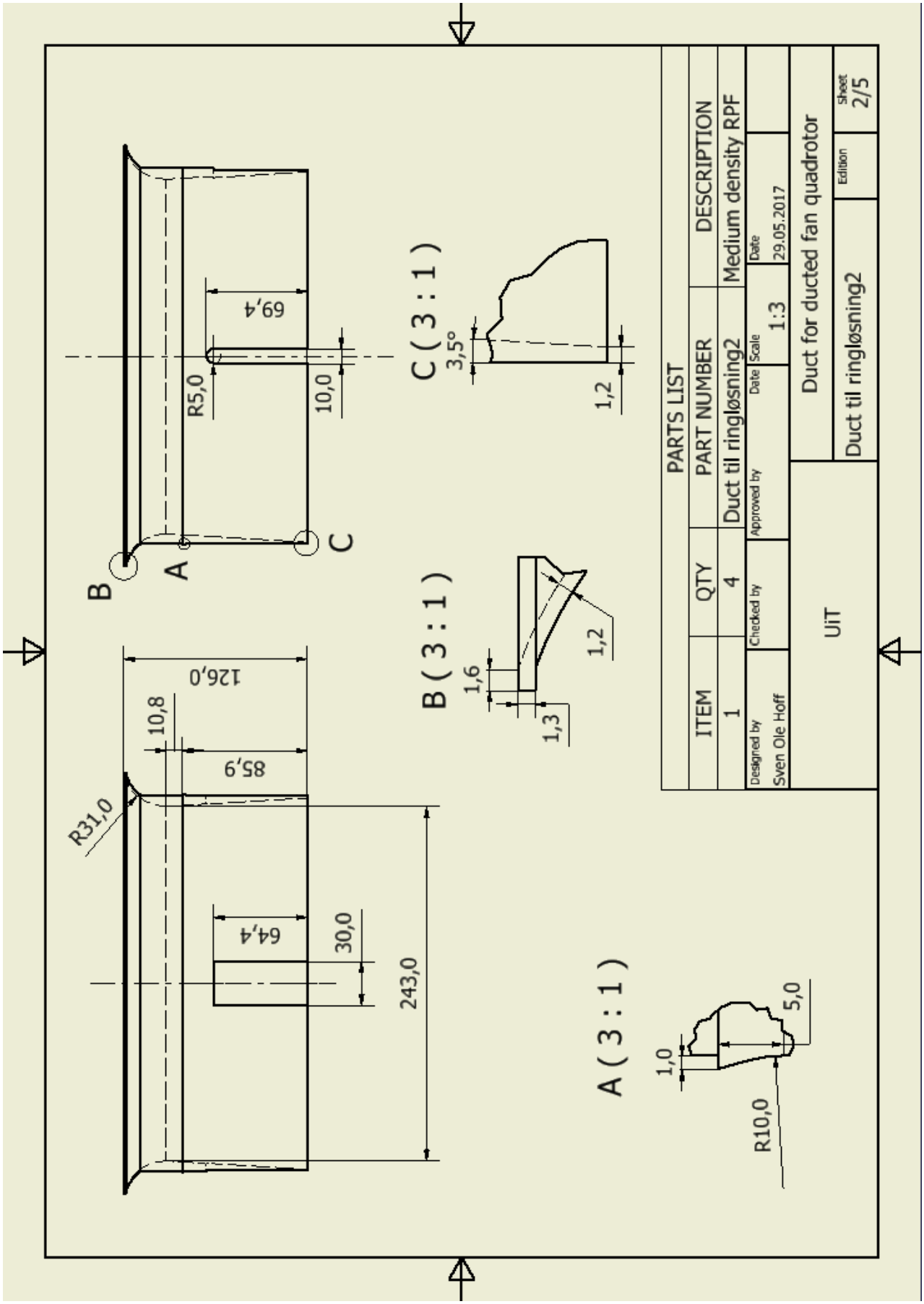

Figure B-2. 2D drawings of duct.

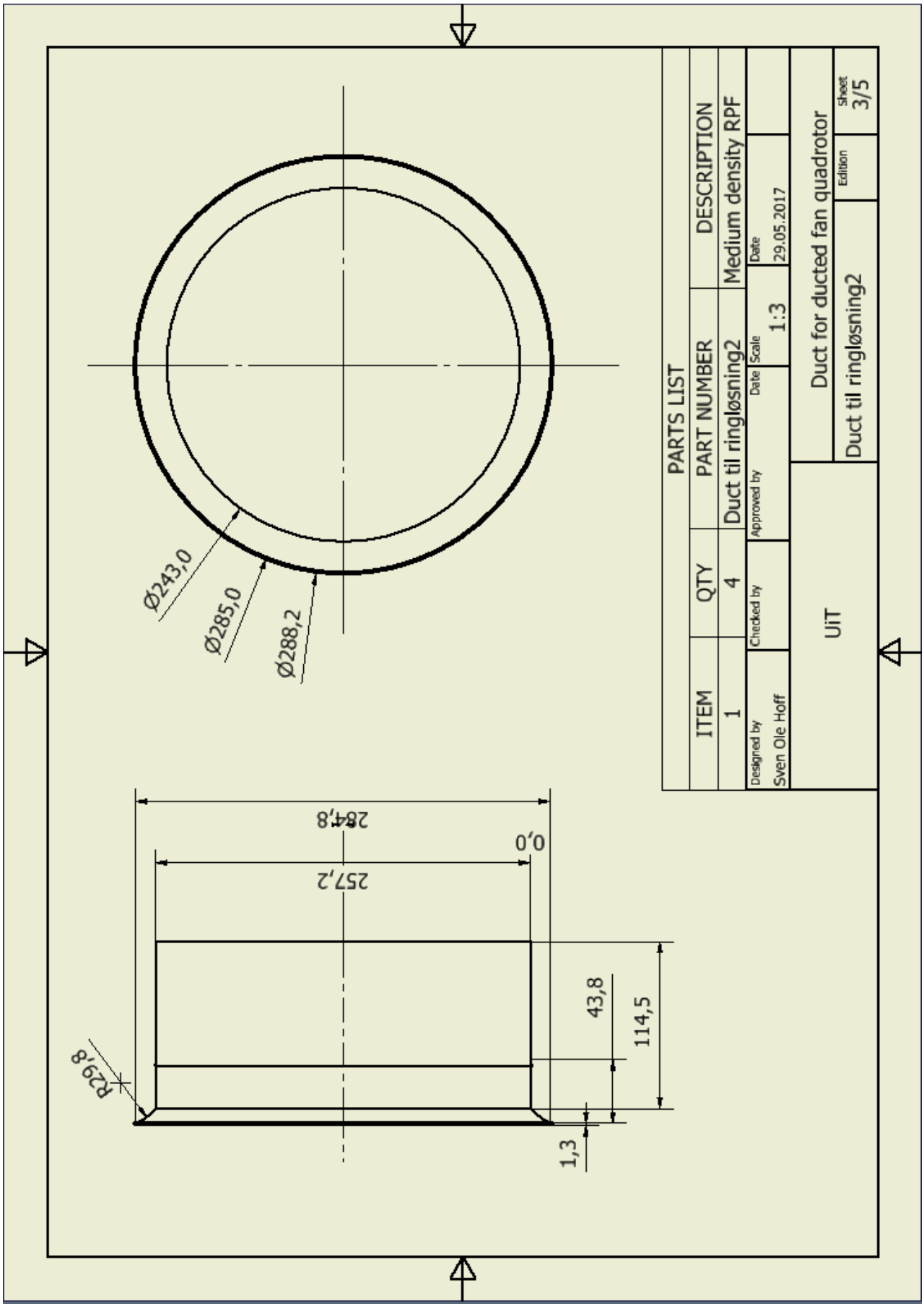

Figure B-4. 2D drawings of duct sheet 2.

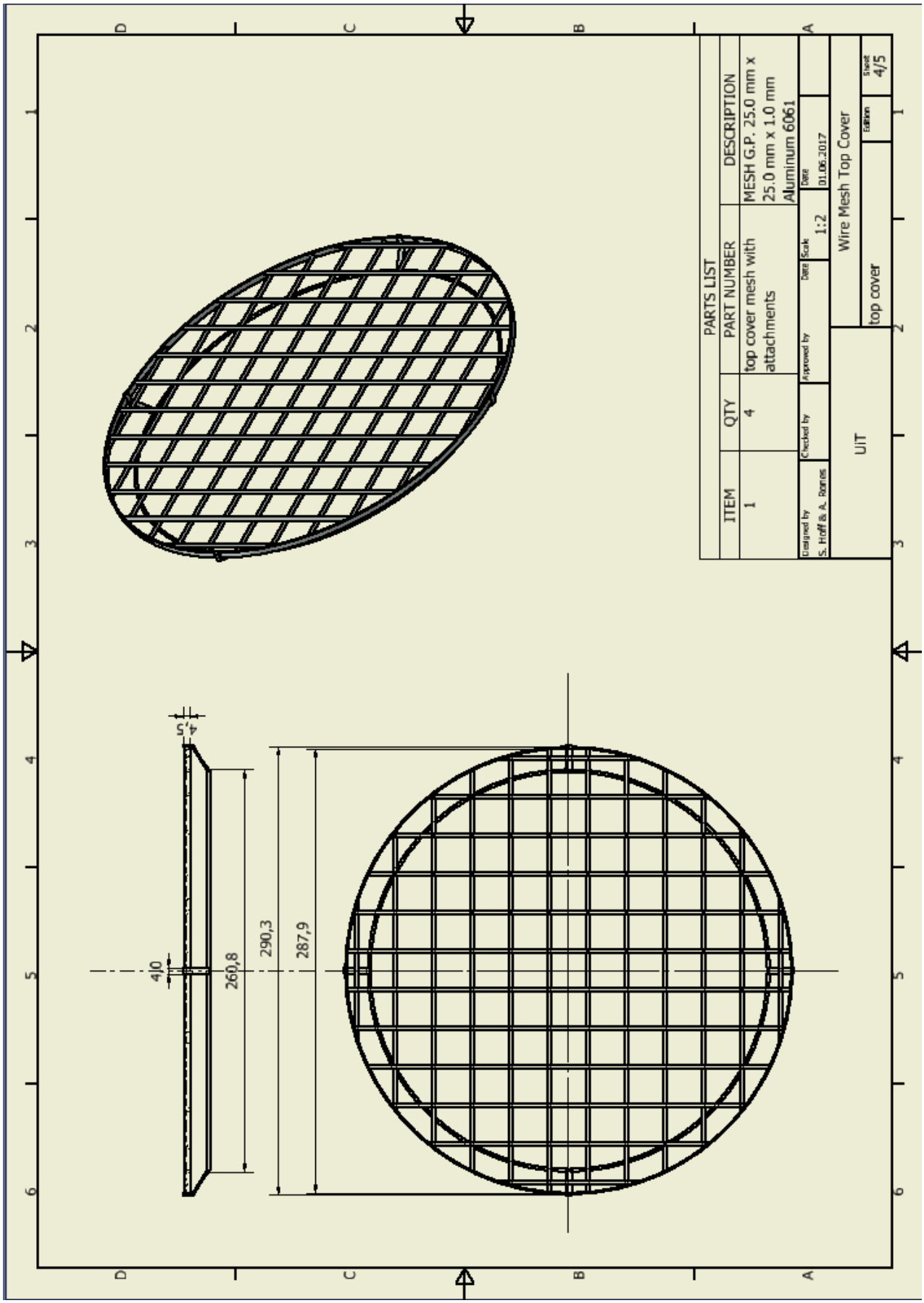

Figure B-4. Wire mesh top cover.

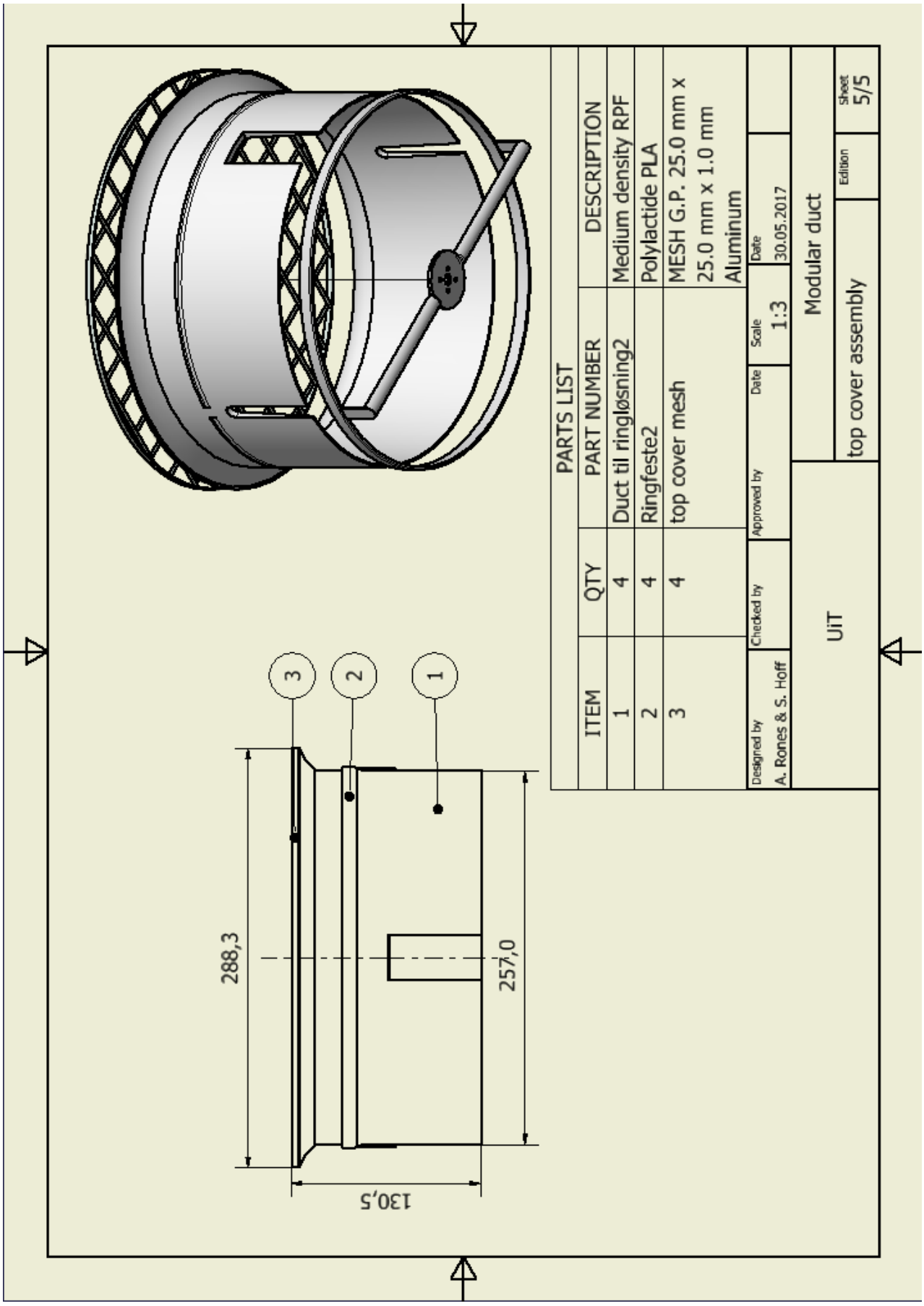

Figure B-5. 2D drawings of the final concept.

C. Thrust values from Balakrishnan's testing.

Table C-1. Thrust at different RPM [1].

S. No.	Thrust N			Speed (rad/s)	Speed (RPM)
	Open quad	Ducted quad	% Increase in Thrust		
1.	0	0	868.0657	0	0
2.	0.26849	2.5991595	489.2652	181.1926	1730
3.	0.476628	2.808603	327.9935	241.4161	2305
4.	0.711847	3.046659	252.0782	295.0324	2817
5.	0.940102	3.309894	196.8804	339.0501	3238
6.	1.202402	3.5696955	158.3813	383.4434	3662
7.	1.512674	3.9084675	122.94	430.0799	4107
8.	1.934366	4.312476	101.631	486.3465	4644
9.	2.405578	4.850391	90.77868	542.3581	5179
10.	2.806378	5.353971	75.258	585.8002	5594
11.	3.348775	5.868996	65.43622	639.9108	6111
12.	3.893492	6.441246	57.54016	689.9952	6589
13.	4.495467	7.082166	52.33853	741.4192	7080
14.	5.047148	7.688751	46.4498	785.5964	7502
15.	5.773696	8.455566	41.51165	840.2401	8024
16.	6.468521	9.153711	40.50327	889.3628	8493
17.	6.514945	9.153711	40.00443	892.5485	8523
18.	6.538158	9.153711	40.00443	894.1372	8538

D. Simulations

Stress analysis

Stress analysis setup

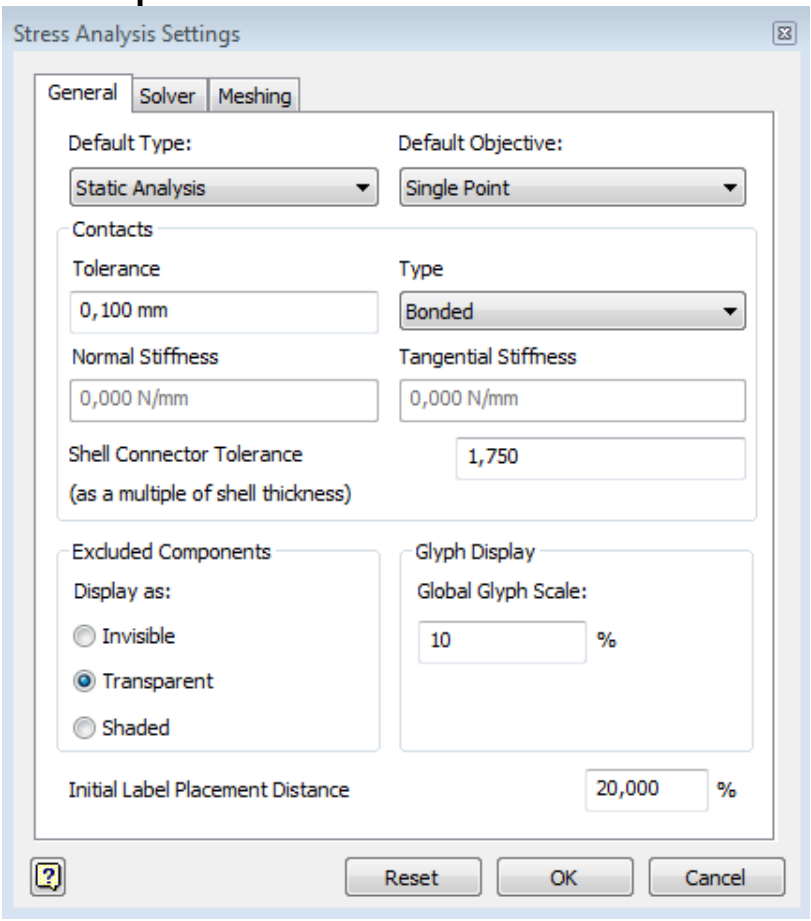

Figure D-1 Stress anlysis, general.

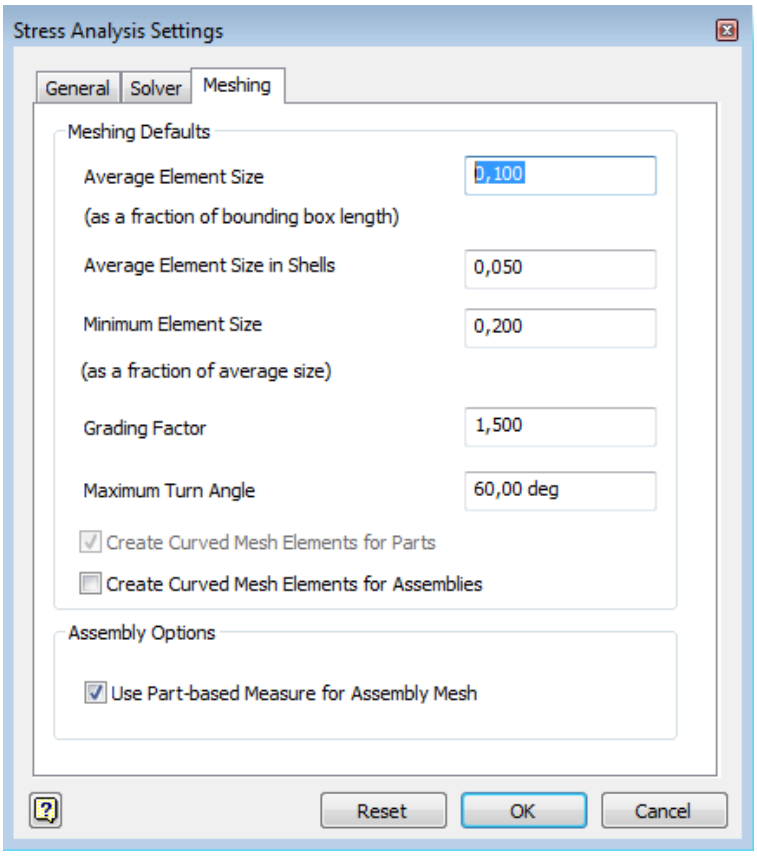

Figure D-2. Stress analysis, meshing.

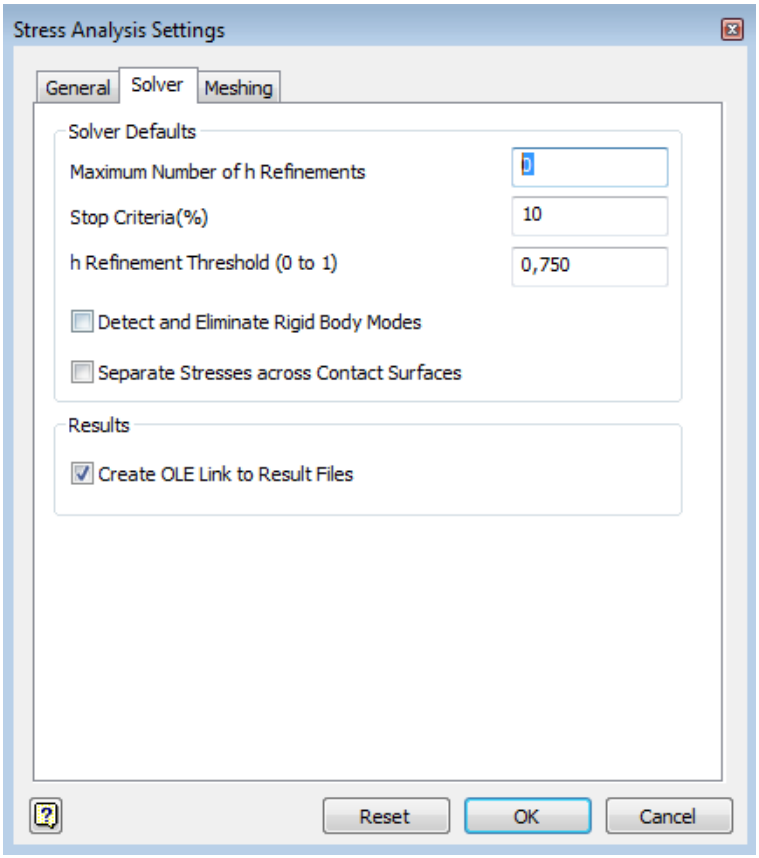

Figure D-3. Stress analysis, solver.

Stress analysis report ring structure

Analyzed File:	Ringfeste2.ipt
Autodesk Inventor Version:	2016 (Build 200138000, 138)
Creation Date:	30.05.2017, 20:05
Simulation Author:	sho114
Summary:	

Project Info (iProperties)

Summary

Author	André

Project

Part Number	Ringfeste2
Designer	André
Cost	kr 0,00
Date Created	04.04.2017

Status

Design Status	WorkInProgress

Physical

Material	ABS Plastic
Density	1,2456 g/cm^3
Mass	0,0332218 kg

Area	34727,1 mm^2
Volume	26671,4 mm^3
Center of Gravity	x=0,00375271 mm y=21,0007 mm z=0,000010765 mm

Note: Physical values could be different from Physical values used by FEA reported below.

Simulation:1

General objective and settings:

Design Objective	Single Point
Simulation Type	Static Analysis
Last Modification Date	30.05.2017, 19:45
Detect and Eliminate Rigid Body Modes	No

Mesh settings:

Avg. Element Size (fraction of model diameter)	0,1
Min. Element Size (fraction of avg. size)	0,2
Grading Factor	1,5
Max. Turn Angle	60 deg
Create Curved Mesh Elements	Yes

Material(s)

Name	ABS Plastic	
General	Mass Density	1,2456 g/cm^3
	Yield Strength	54,9995 MPa

	Ultimate Tensile Strength	46,9947 MPa
Stress	Young's Modulus	3,30259 GPa
	Poisson's Ratio	0,38 ul
	Shear Modulus	1,19659 GPa
Part Name(s)	Ringfeste2.ipt	

Operating conditions

Gravity

Load Type	Gravity
Magnitude	14920,000 mm/s^2
Vector X	0,000 mm/s^2
Vector Y	-14920,000 mm/s^2
Vector Z	0,000 mm/s^2

Selected Face(s)

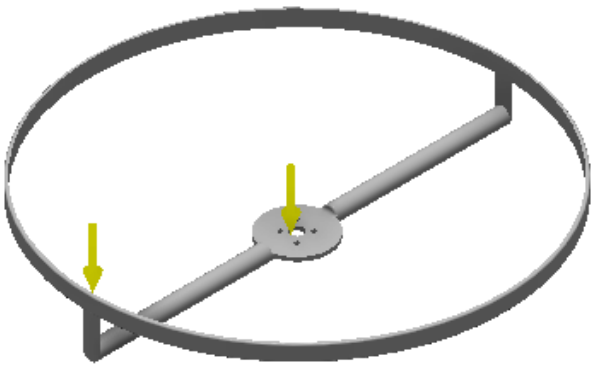

Force:1

Load Type	Force
Magnitude	1,067 N
Vector X	0,000 N
Vector Y	-1,067 N
Vector Z	0,000 N

Selected Face(s)

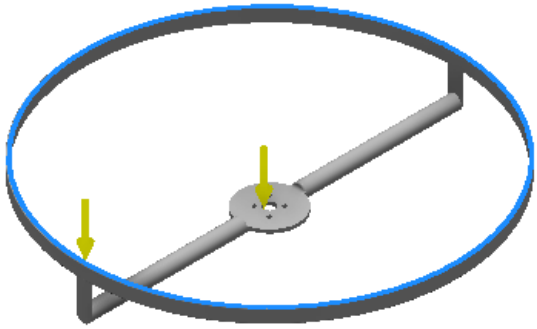

Fixed Constraint:1

Constraint Type	Fixed Constraint

Selected Face(s)

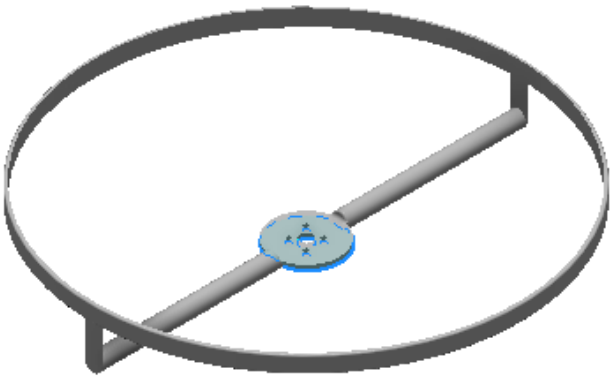

Results

Reaction Force and Moment on Constraints

Constraint Name	Reaction Force		Reaction Moment	
	Magnitude	Component (X,Y,Z)	Magnitude	Component (X,Y,Z)
Fixed Constraint:1	1,56954 N	0 N	0,00134275 N m	0 N m
		1,56954 N		0 N m
		0 N		0,00134275 N m

Result Summary

Name	Minimum	Maximum
Volume	26672,6 mm^3	
Mass	0,0332233 kg	
Von Mises Stress	0,000227086 MPa	10,5575 MPa
1st Principal Stress	-5,63905 MPa	8,57468 MPa
3rd Principal Stress	-12,964 MPa	1,3255 MPa

Displacement	0 mm	2,37515 mm
Safety Factor	5,2095 ul	15 ul

Figures

Von Mises Stress

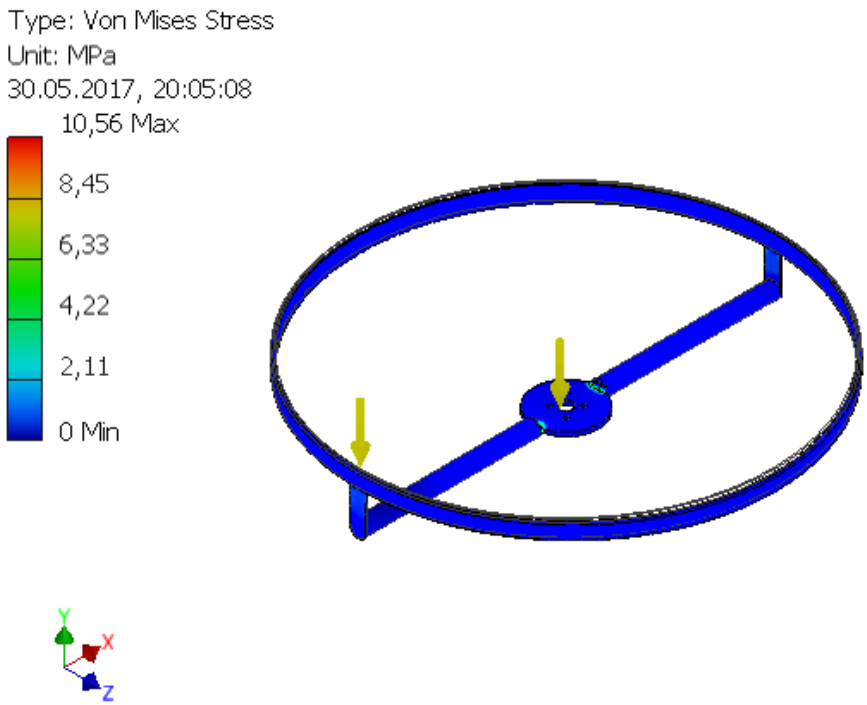

1st Principal Stress

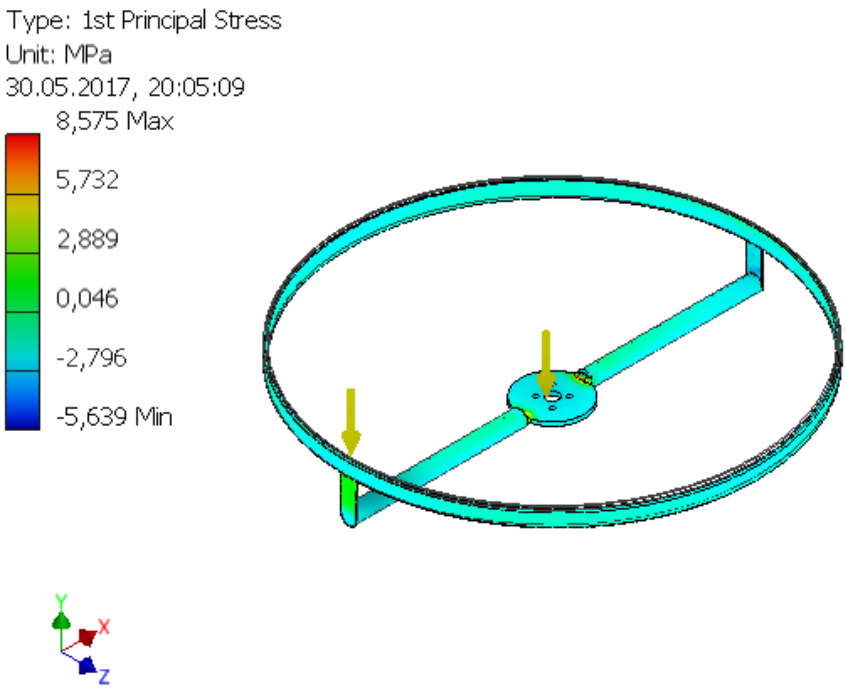

3rd Principal Stress

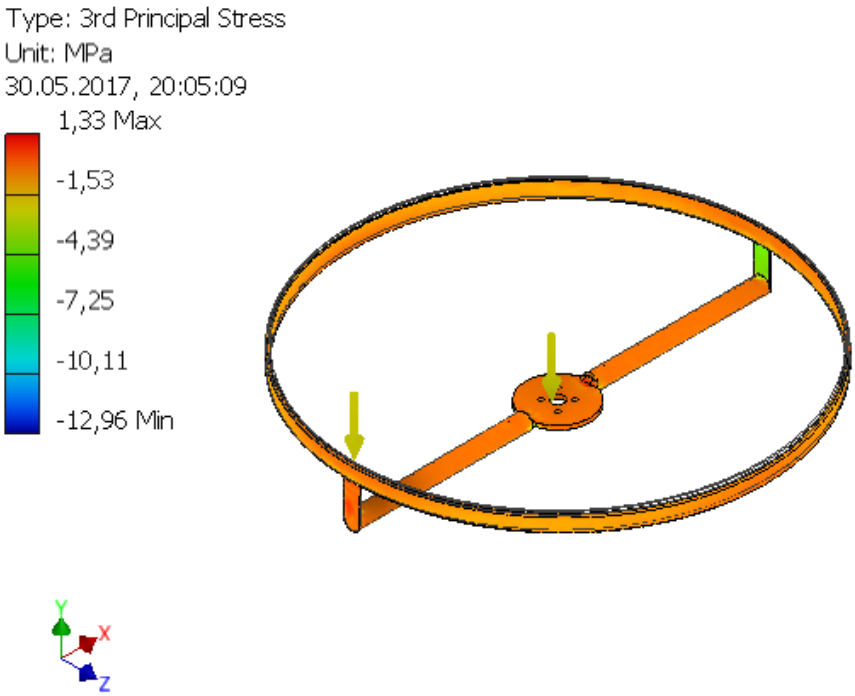

Displacement

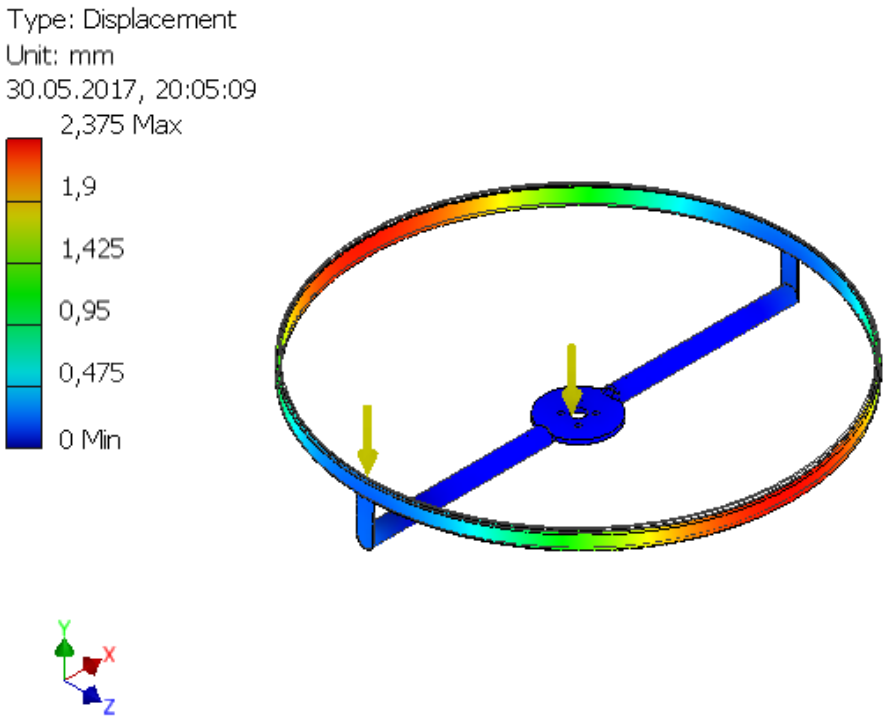

Safety Factor

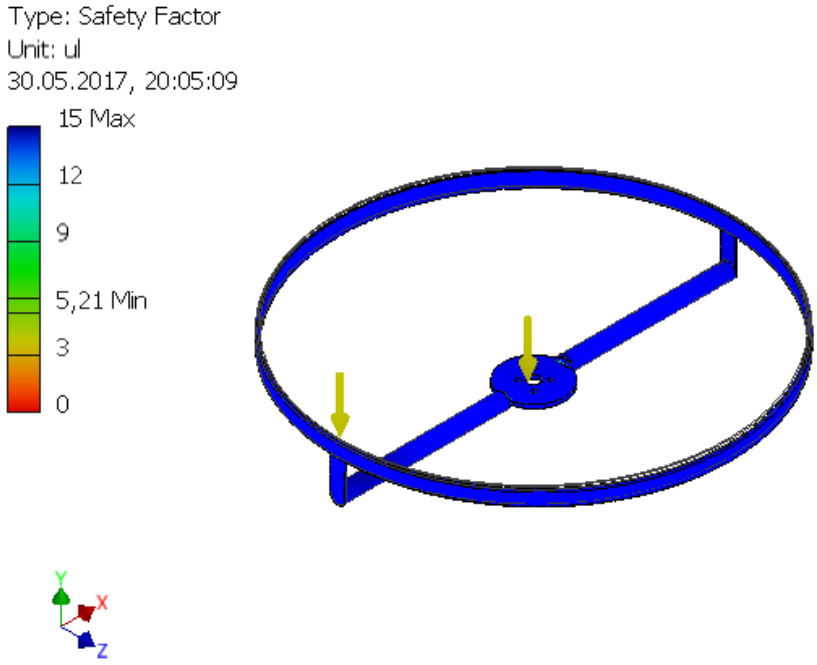

Stress analysis report Duct

Analyzed File:	Duct til ringløsning2.ipt
Autodesk Inventor Version:	2016 (Build 200138000, 138)
Creation Date:	31.05.2017, 14:33
Simulation Author:	sho114
Summary:	

Project Info (iProperties)

Summary

Title	Arm integrert.STEP

Project

Part Number	Duct til ringløsning2
Description	STEP AP214
Revision Number	ANY
Designer	sho114
Cost	kr 0,00
Date Created	28.02.2017

Status

Design Status	WorkInProgress

Physical

Material	Polystyrene

Density	0,0775037 g/cm^3
Mass	0,0313935 kg
Area	215140 mm^2
Volume	405058 mm^3
Center of Gravity	x=1,94752 mm y=-25,0874 mm z=0 mm

Note: Physical values could be different from Physical values used by FEA reported below.

Simulation:1

General objective and settings:

Design Objective	Single Point
Simulation Type	Static Analysis
Last Modification Date	31.05.2017, 13:21
Detect and Eliminate Rigid Body Modes	No

Mesh settings:

Avg. Element Size (fraction of model diameter)	0,1
Min. Element Size (fraction of avg. size)	0,2
Grading Factor	1,5
Max. Turn Angle	60 deg
Create Curved Mesh Elements	Yes

Material(s)

Name	Polystyrene	
General	Mass Density	0,0775037 g/cm^3
	Yield Strength	3,49978 MPa
	Ultimate Tensile Strength	5,10212 MPa
Stress	Young's Modulus	0,199996 GPa
	Poisson's Ratio	0,33 ul
	Shear Modulus	0,0751866 GPa
Part Name(s)	Duct til ringløsning2.ipt	

Operating conditions

Gravity

Load Type	Gravity
Magnitude	14920,000 mm/s^2
Vector X	0,000 mm/s^2
Vector Y	-14920,000 mm/s^2
Vector Z	0,000 mm/s^2

Selected Face(s)

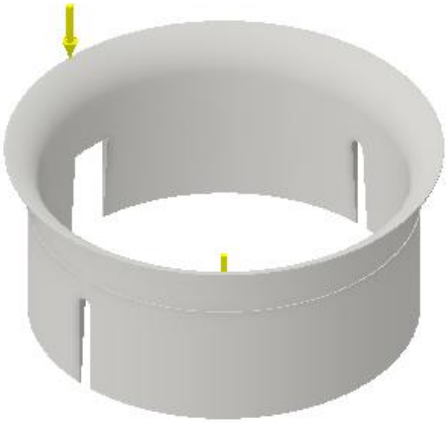

Force:1

Load Type	Force
Magnitude	1,200 N
Vector X	0,000 N
Vector Y	-1,200 N
Vector Z	0,000 N

Selected Face(s)

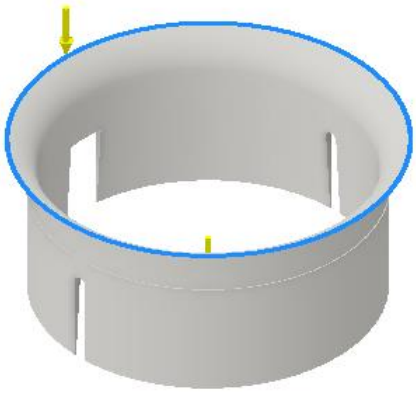

Fixed Constraint:1

Constraint Type	Fixed Constraint

Selected Face(s)

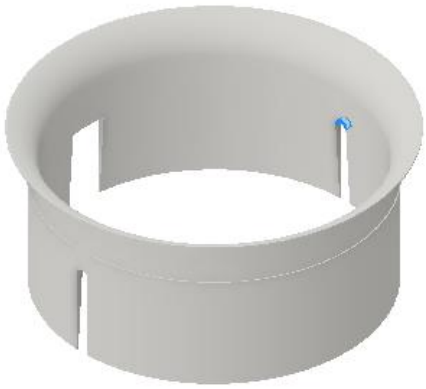

Fixed Constraint:2

Constraint Type	Fixed Constraint

Selected Face(s)

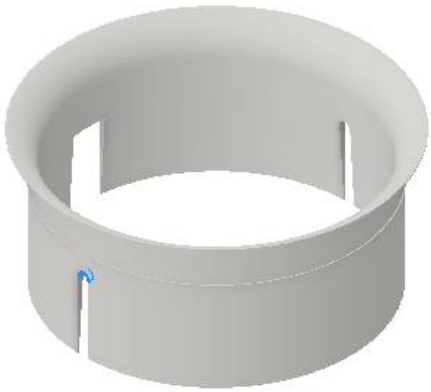

Results

Reaction Force and Moment on Constraints

Constraint Name	Reaction Force		Reaction Moment	
	Magnitude	Component (X,Y,Z)	Magnitude	Component (X,Y,Z)
Fixed Constraint:1	0,837366 N	0 N	0,0135202 N m	-0,0135039 N m
		0,834702 N		-0,0000496911 N m
		0,0667459 N		0,000661315 N m
Fixed Constraint:2	0,837589 N	0 N	0,0135044 N m	0,0134841 N m
		0,834935 N		0,0000281207 N m
		-0,0666207 N		0,000739585 N m

Result Summary

Name	Minimum	Maximum
Volume	405058 mm^3	
Mass	0,0313935 kg	
Von Mises Stress	0,0000579012 MPa	0,135268 MPa
1st Principal Stress	-0,091042 MPa	0,176114 MPa
3rd Principal Stress	-0,23364 MPa	0,067006 MPa
Displacement	0 mm	0,146755 mm
Safety Factor	15 ul	15 ul

Figures

Von Mises Stress

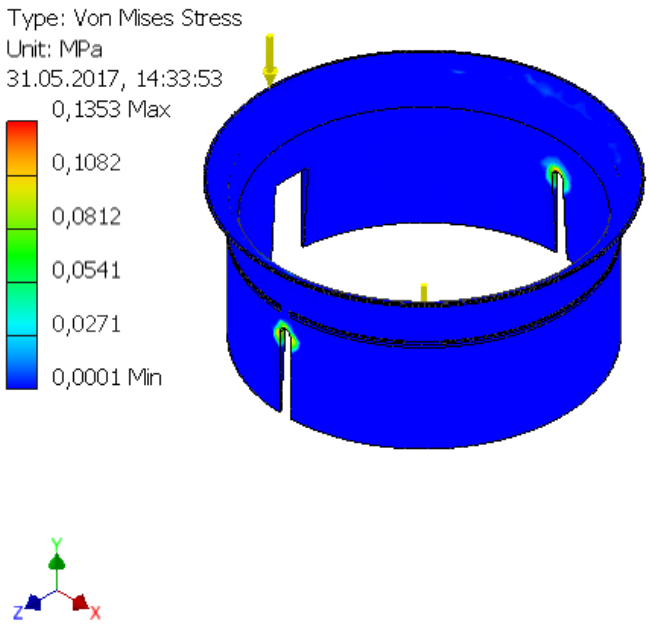

1st Principal Stress

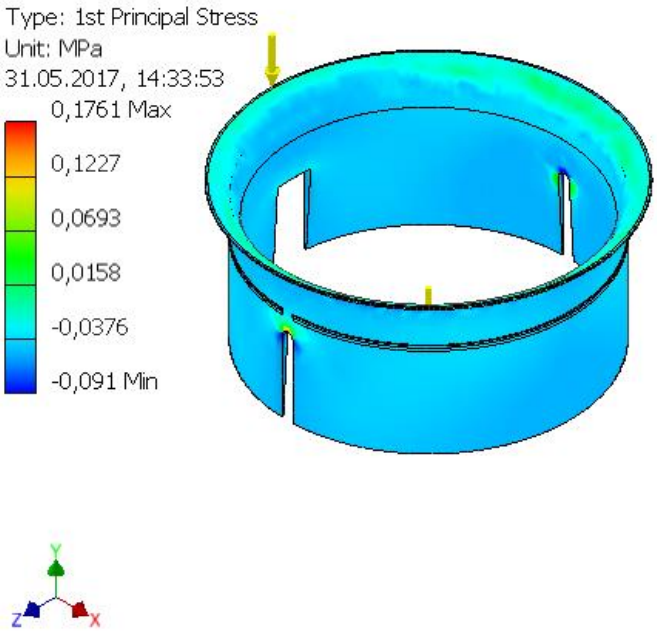

3rd Principal Stress

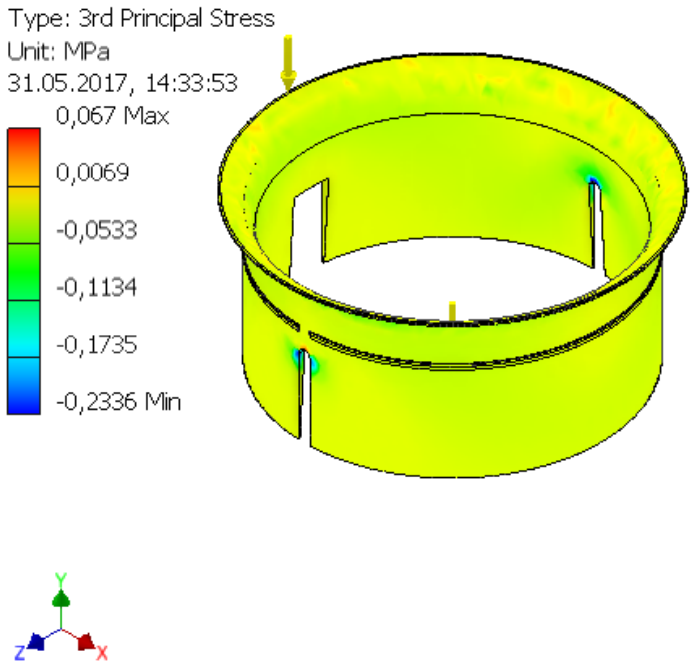

Displacement

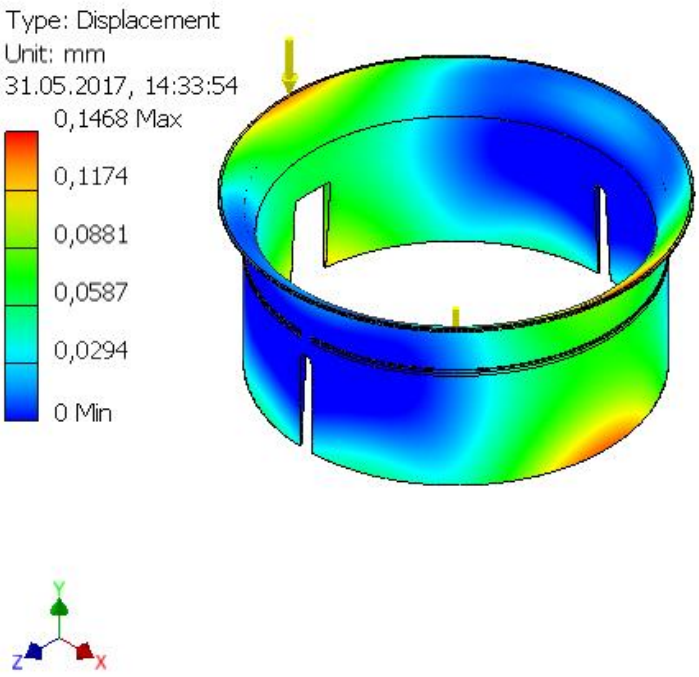

Safety Factor

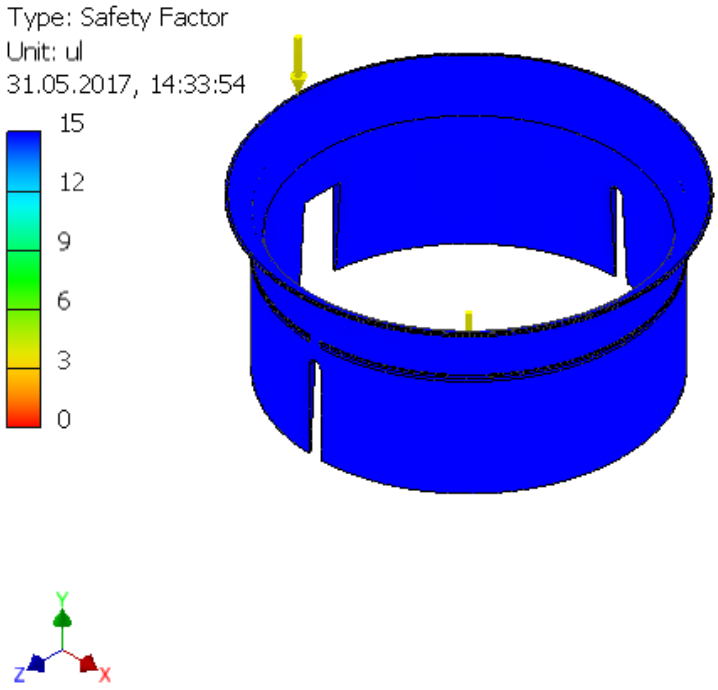

Stress analysis report of whole structure

Analyzed File:	top cover assembly.iam
Autodesk Inventor Version:	2016 (Build 200138000, 138)
Creation Date:	31.05.2017, 14:49
Simulation Author:	sho114
Summary:	

Project Info (iProperties)

Summary

Author	aro083

Project

Part Number	top cover assembly
Designer	aro083
Cost	kr 0,00
Date Created	29.05.2017

Status

Design Status	WorkInProgress

Physical

Mass	0,145438 kg
Area	300177 mm^2
Volume	461664 mm^3

Center of Gravity	x=-9,54852 mm y=6,09382 mm z=-0,000485585 mm

Note: Physical values could be different from Physical values used by FEA reported below.

Simulation:1

General objective and settings:

Design Objective	Single Point
Simulation Type	Static Analysis
Last Modification Date	31.05.2017, 14:45
Detect and Eliminate Rigid Body Modes	No
Separate Stresses Across Contact Surfaces	No
Motion Loads Analysis	No

Mesh settings:

Avg. Element Size (fraction of model diameter)	0,1
Min. Element Size (fraction of avg. size)	0,2
Grading Factor	1,5
Max. Turn Angle	60 deg
Create Curved Mesh Elements	No
Use part based measure for Assembly mesh	Yes

Material(s)

Name	Polystyrene

General	Mass Density	0,0775037 g/cm^3
	Yield Strength	3,49978 MPa
	Ultimate Tensile Strength	5,10212 MPa
Stress	Young's Modulus	0,199996 GPa
	Poisson's Ratio	0,33 ul
	Shear Modulus	0,0751866 GPa
Part Name(s)	Duct til ringløsning2.ipt	

Name	ABS Plastic	
General	Mass Density	1,2456 g/cm^3
	Yield Strength	54,9995 MPa
	Ultimate Tensile Strength	46,9947 MPa
Stress	Young's Modulus	3,30259 GPa
	Poisson's Ratio	0,38 ul
	Shear Modulus	1,19659 GPa
Part Name(s)	Ringfeste2.ipt	

Name	Aluminum 6061	
General	Mass Density	2,7 g/cm^3
	Yield Strength	275 MPa
	Ultimate Tensile Strength	310 MPa
Stress	Young's Modulus	68,9 GPa
	Poisson's Ratio	0,33 ul
	Shear Modulus	25,9023 GPa

Part Name(s)	top cover mesh.ipt

Operating conditions

Gravity

Load Type	Gravity
Magnitude	14920,000 mm/s^2
Vector X	0,000 mm/s^2
Vector Y	-14920,000 mm/s^2
Vector Z	0,000 mm/s^2

Selected Face(s)

Fixed Constraint:1

Constraint Type	Fixed Constraint

Selected Face(s)

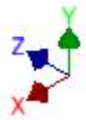

Contacts (Bonded)

Name	Part Name(s)
Bonded:1	Duct til ringløsning2:1 Ringfeste2:1
Bonded:2	Duct til ringløsning2:1 Ringfeste2:1
Bonded:3	Duct til ringløsning2:1 Ringfeste2:1
Bonded:4	Duct til ringløsning2:1 Ringfeste2:1

Bonded:5	Duct til ringløsning2:1 Ringfeste2:1
Bonded:6	Duct til ringløsning2:1 top cover mesh:1
Bonded:7	Duct til ringløsning2:1 top cover mesh:1
Bonded:8	Duct til ringløsning2:1 top cover mesh:1
Bonded:9	Duct til ringløsning2:1 top cover mesh:1
Bonded:10	Duct til ringløsning2:1 top cover mesh:1
Bonded:11	Duct til ringløsning2:1 top cover mesh:1
Bonded:12	Duct til ringløsning2:1 top cover mesh:1
Bonded:13	Duct til ringløsning2:1 top cover mesh:1
Bonded:14	Duct til ringløsning2:1 top cover mesh:1
Bonded:15	Duct til ringløsning2:1 top cover mesh:1
Bonded:16	Duct til ringløsning2:1 top cover mesh:1
Bonded:17	Duct til ringløsning2:1 top cover mesh:1
Bonded:18	Duct til ringløsning2:1 top cover mesh:1
Bonded:19	Duct til ringløsning2:1 Ringfeste2:1

Bonded:20	Duct til ringløsning2:1 Ringfeste2:1

Results

Reaction Force and Moment on Constraints

Constraint Name	Reaction Force		Reaction Moment	
	Magnitude	Component (X,Y,Z)	Magnitude	Component (X,Y,Z)
Fixed Constraint:1	2,04495 N	0 N	0,00115446 N m	-0,00115446 N m
		2,04495 N		0 N m
		0 N		0 N m

Result Summary

Name	Minimum	Maximum
Volume	461664 mm^3	
Mass	0,145438 kg	
Von Mises Stress	0,0000441835 MPa	9,25216 MPa
1st Principal Stress	-2,39125 MPa	10,3239 MPa
3rd Principal Stress	-11,165 MPa	1,99646 MPa
Displacement	0 mm	0,387195 mm
Safety Factor	7,22668 ul	15 ul
Contact Pressure	0 MPa	16,9355 MPa
Contact Pressure X	-2,12996 MPa	1,34424 MPa
Contact Pressure Y	-2,22791 MPa	4,25884 MPa
Contact Pressure Z	-16,6096 MPa	14,293 MPa

Figures

Von Mises Stress

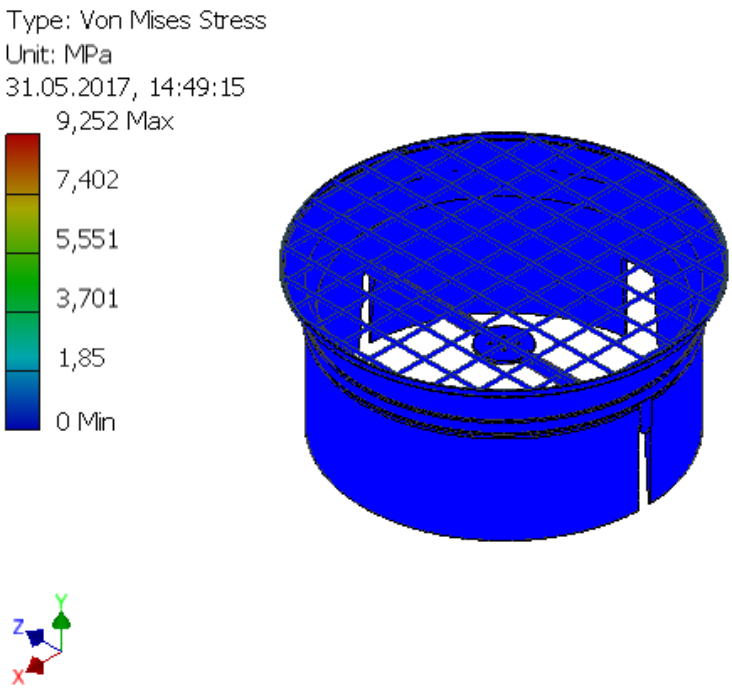

1st Principal Stress

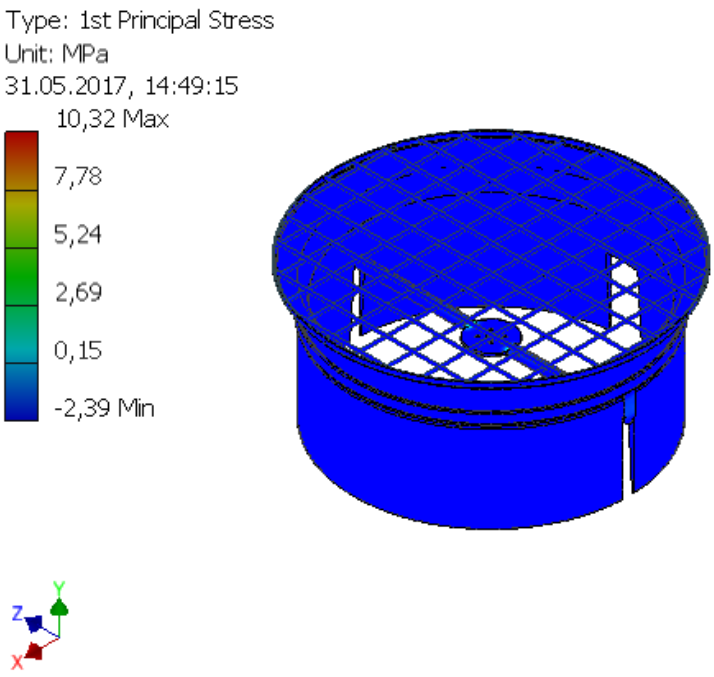

3rd Principal Stress

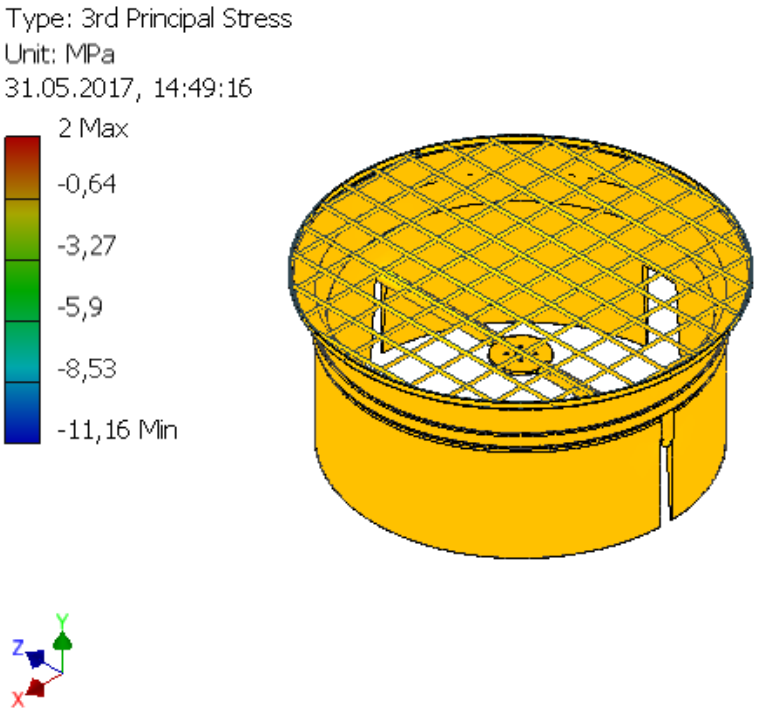

Displacement

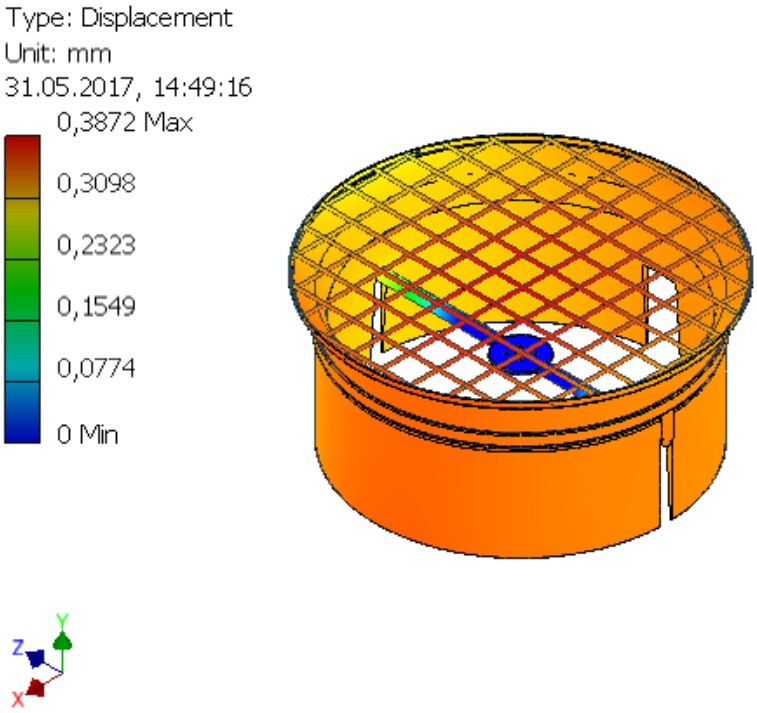

Safety Factor

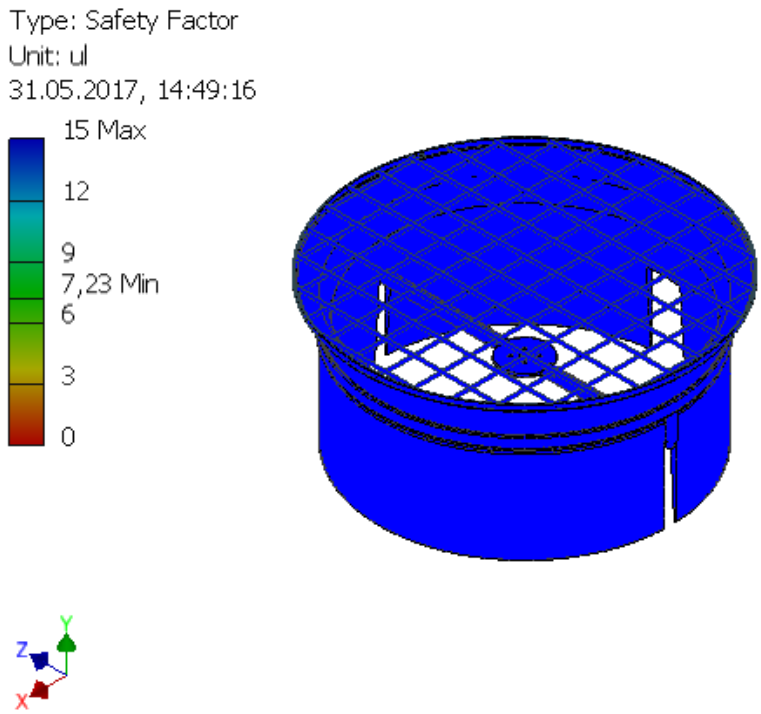

Contact Pressure

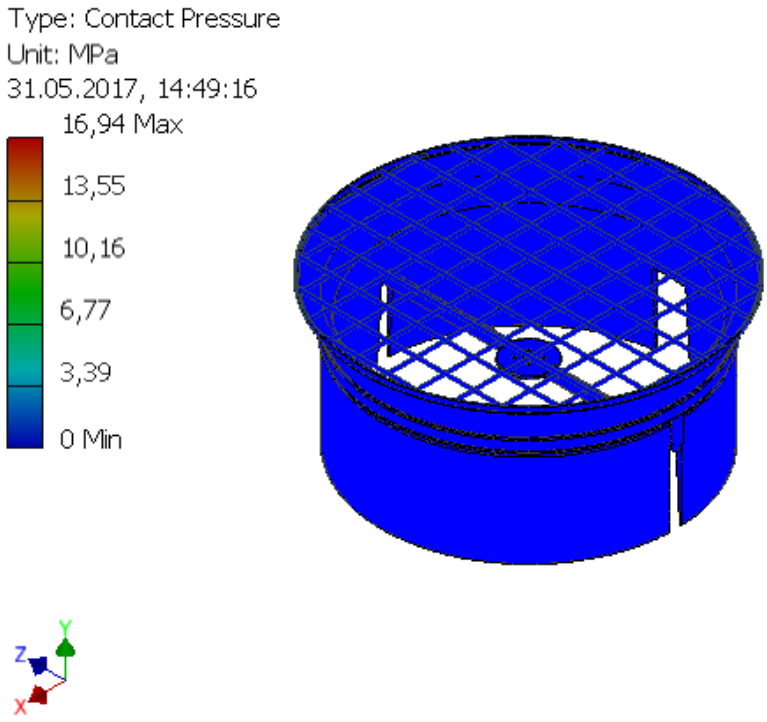

Contact Pressure X

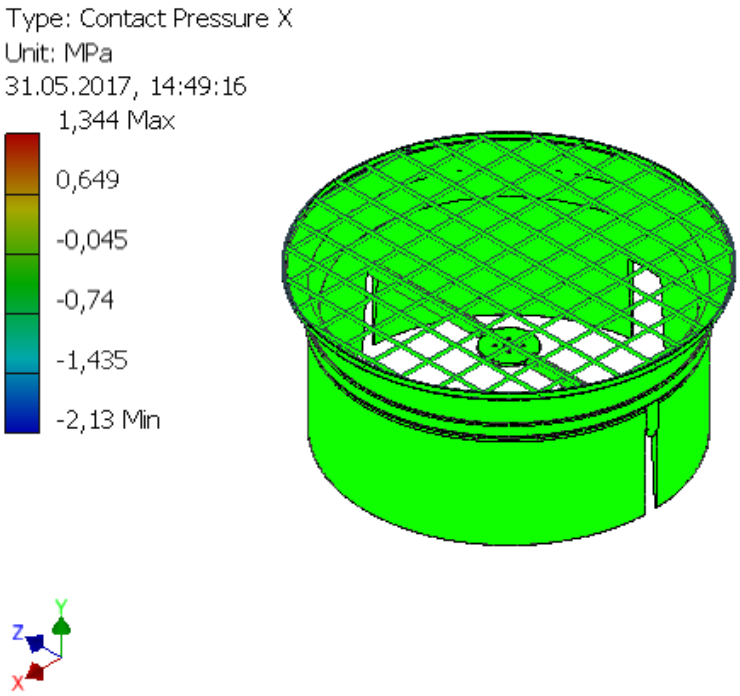

Contact Pressure Y

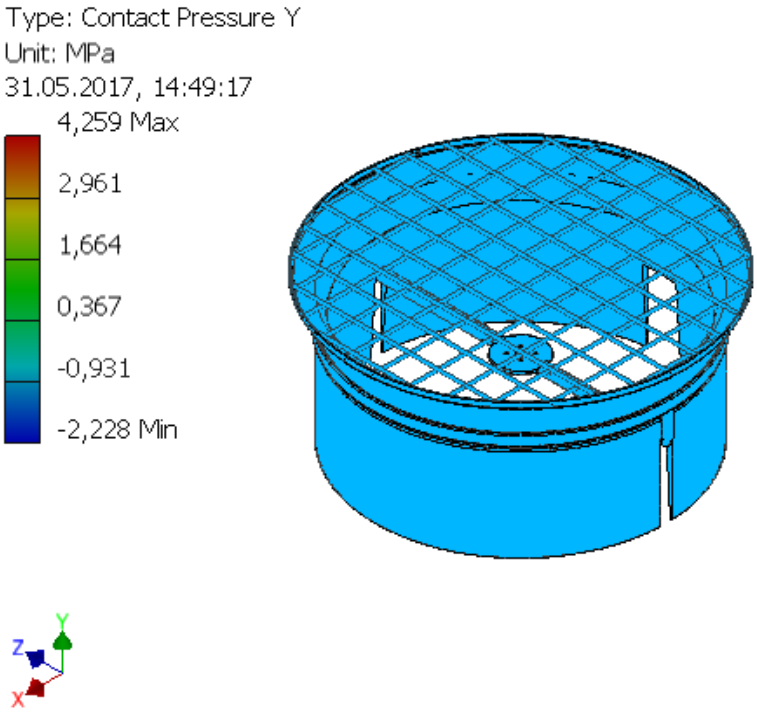

Contact Pressure Z

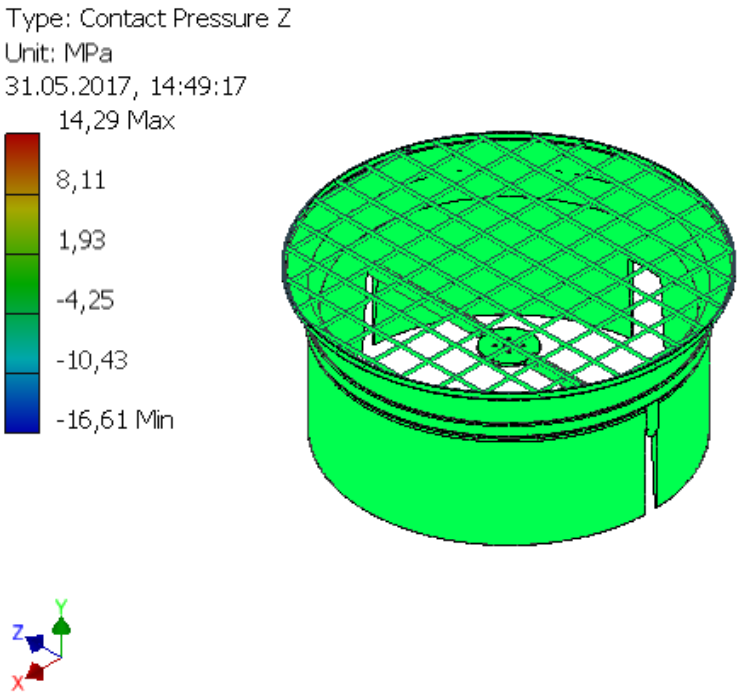

E. Prototype

Pictures from prototype production